JCB Journal of Cell Biology

ARTICLE

CaMKII mediates sexually dimorphic synaptic transmission at neuromuscular junctions in *C. elegans*

Wan-Xin Zeng[1,2,3*], Haowen Liu[4*], Yue Hao[1,2,3*], Kang-Ying Qian[1,2,3], Fu-Min Tian[1], Lei Li[4], Bin Yu[5], Xian-Ting Zeng[1], Shangbang Gao[5], Zhitao Hu[4,6], and Xia-Jing Tong[1]

Sexually dimorphic behaviors are ubiquitous throughout the animal kingdom. Although both sex-specific and sex-shared neurons have been functionally implicated in these diverse behaviors, less is known about the roles of sex-shared neurons. Here, we discovered sexually dimorphic cholinergic synaptic transmission in *C. elegans* occurring at neuromuscular junctions (NMJs), with males exhibiting increased release frequencies, which result in sexually dimorphic locomotion behaviors. Scanning electron microscopy revealed that males have significantly more synaptic vesicles (SVs) at their cholinergic synapses than hermaphrodites. Analysis of previously published transcriptome identified the male-enriched transcripts and focused our attention on UNC-43/CaMKII. We ultimately show that differential accumulation of UNC-43 at cholinergic neurons controls axonal SV abundance and synaptic transmission. Finally, we demonstrate that sex reversal of all neurons in hermaphrodites generates male-like cholinergic transmission and locomotion behaviors. Thus, beyond demonstrating UNC-43/CaMKII as an essential mediator of sex-specific synaptic transmission, our study provides molecular and cellular insights into how sex-shared neurons can generate sexually dimorphic locomotion behaviors.

Introduction

Biological sex exerts a profound influence on animal behaviors. Sexually dimorphic behaviors, including mate-seeking, courtship, and parental care, play essential roles in animals' survival and maintenance of the generations (Cline and Meyer, 1996; Kelley, 1988; Peedikayil-Kurien et al., 2022). While some sex differences in behaviors are acquired through experience, innate behaviors such as mating and aggression do not require prior training or experience (Asahina et al., 2014; Cachero et al., 2010). Furthermore, many psychiatric disorders also show a sexually dimorphic prevalence. For instance, autism spectrum disorder (ASD) affects human males at a rate four to five times higher than females (Hiller et al., 2016; Van Wijngaarden-Cremers et al., 2014), whereas major depressive disorder (MDD) is more prevalent in human females (Kessler et al., 1993). However, our understanding of the molecular and cellular mechanisms underlying these sex-specific behaviors remains limited.

Animal behaviors are mediated by reliable synaptic transmission within the nervous system, and its disturbance has been linked with many psychiatric disorders, such as ASD and MDD (Bourgeron, 2015; Howard et al., 2018; Iossifov et al., 2012; Kang et al., 2012; Lima Caldeira et al., 2019; Ohgi et al., 2015). Thus, understanding and identification of the sexually dimorphic synaptic transmission can provide valuable insights into sex differences in behaviors and shed light on the pathophysiology of psychiatric disorders. Sexually dimorphic synaptic transmissions may arise from sex-specific neurons or potentially from sex-shared neurons that undergo sex-specific differentiation (Cachero et al., 2010; Emmons, 2018; García and Portman, 2016; Hart and Hobert, 2015; Simerly, 2002). However, less has been done with sex-shared neurons, although it is known that they are strongly sexually dimorphic in their synaptic connectivity patterns. In *C. elegans*, the PHB phasmid sensory neurons undergo sex-specific pruning via the ubiquitin pathway, resulting in the formation of sex-specific synapses (Oren-Suissa et al., 2016; Salzberg et al., 2020). Additionally, the sensory neuron pair PHC differentiates into a male-specific densely connected hub sensory neuron/interneuron (Serrano-Saiz et al., 2017). In mammals, a previous study showed that sex-shared GABAergic neurons in the medial amygdala display sexually

[1]School of Life Science and Technology, ShanghaiTech University, Shanghai, China; [2]Institute of Neuroscience, Shanghai Institutes for Biological Sciences, Chinese Academy of Sciences, Shanghai, China; [3]University of Chinese Academy of Sciences, Beijing, China; [4]Queensland Brain Institute, Clem Jones Centre for Ageing Dementia Research (CJCADR), The University of Queensland, Brisbane, Australia; [5]College of Life Science and Technology, Huazhong University of Science and Technology, Wuhan, China; [6]Department of Neuroscience, City University of Hong Kong, Kowloon, China.

*W.-X. Zeng, H. Liu, and Y. Hao contributed equally to this paper. Correspondence to Zhitao Hu: z.hu1@uq.edu.au; Xia-Jing Tong: tongxj@shanghaitech.edu.cn.

dimorphic features: activation of this population of neurons in females promotes parental behavior, while activation of this population in males promotes infanticidal behavior (in an activity-level-dependent manner; Chen et al., 2019). However, the underlying molecular mechanism remains elusive.

The process of synaptic transmission involves several steps: neurotransmitter synthesis and packaging into synaptic vesicles (SVs), upon calcium influx mediated by the voltage-gated calcium channel, docking and fusing of SVs with presynaptic membranes for neurotransmitters release, and binding of neurotransmitters to the postsynaptic receptors to hyperpolarize or depolarize postsynaptic cells. In theory, there could be sex-specific characteristics related to SV biogenesis, SV docking/fusion, and/or postsynaptic receptor abundance that result in sexually dimorphic synaptic transmission. However, considering the complexity of the vertebrate nervous system, it is challenging to dissect and compare individual neuron types between the two sexes to study sexually dimorphic synaptic transmission processes. Thus, simpler model organisms such as *Drosophila* and *Caenorhabditis elegans* (*C. elegans*) provide excellent models for studying sexual dimorphism in the nervous system.

In *C. elegans*, there are two sexes: somatic female hermaphrodites and males. Hermaphrodites have eight sex-specific neurons contributing to egg-laying behaviors, while males have 93 sex-specific neurons subserving copulation and other male-specific behaviors. Besides that, both sexes possess 294 sex-shared neurons (Cook et al., 2019). However, only a limited number of molecular and/or synaptic transmission features have been associated with sex-shared but sexually dimorphic neurons and synapses. The *C. elegans* hermaphrodites and males exhibit sexually dimorphic motor behaviors: the males present faster locomotion velocity and a more substantial body wave curvature (Mowrey et al., 2014). The sinusoidal movement is mediated by alternative excitation and inhibition of the body-wall muscle by the neuromuscular junctions (NMJs), suggesting that sexually dimorphic differentiation or connections may exist at the NMJs in *C. elegans*.

Here, we show that in *C. elegans*, cholinergic synaptic transmission at NMJs is significantly more frequent in males than in hermaphrodites, and we demonstrate sexually dimorphic cholinergic transmission at NMJs, which emerges during the L4 stage, when male sexual structures develop. Our scanning electron microscopy analysis of synapse ultrastructure revealed that males have dramatically more synaptic vesicles (SVs) and dense core vesicles (DCVs) at cholinergic motor neuron terminals compared with hermaphrodites. Further, analysis of the temporal gene expression profiles in the two sexes identified the male-enriched transcripts expressed in cholinergic motor neurons, including UNC-43/CaMKII. UNC-43/CaMKII is highly expressed in males in cholinergic motor neurons, but not in GABAergic motor neurons. Given the established role of CaMKII in SVs and DCVs biogenesis, this differential expression pattern can plausibly explain the sex-specific SVs abundance, differential cholinergic synaptic transmission, and distinct locomotor behaviors of the two sexes. Finally, we demonstrate that pan-neuronal masculinization in hermaphrodites causes male-like higher cholinergic transmission and hyper locomotor activity.

Results

Sexually dimorphic NMJ synaptic transmission and locomotion behaviors in *C. elegans*

C. elegans has two sexes: hermaphrodites (somatic females) and males, and they display distinct patterns in shared behaviors such as locomotion (Mowrey et al., 2014). Previous studies have characterized differences in both the dynamics and geometry of locomotion between hermaphrodites and males (Mowrey et al., 2014). We experimentally confirmed that (i) both sexes display sinusoidal movement when crawling on an agar gel surface (Fig. 1 A) and (ii) males showed more prominent body wave curvature and had faster wave speed (Fig. 1, B–D). Beyond this previously known dimorphism, we also detected a behavioral difference during swimming in liquid culture: specifically, the male thrashing frequency was significantly higher than that of hermaphrodites (Fig. 1 E).

Locomotion behaviors in *C. elegans* are known to be controlled by neuromuscular junctions (NMJs), which comprise body-wall muscles that are innervated by excitatory cholinergic and inhibitory GABAergic motor neurons (Richmond and Jorgensen, 1999). The sex-specific locomotion behaviors prompted us to test whether the NMJ synaptic transmission differs between the two sexes. We performed the aldicarb assay to measure the excitatory and inhibitory transmission ratio (E/I ratio) at NMJs in the two sexes (Mahoney et al., 2006). Aldicarb is an acetylcholinesterase inhibitor, and exposure of *C. elegans* to aldicarb results in the accumulation of acetylcholine, muscle overexcitation, and worm paralysis. The timing of paralysis is also influenced by inhibitory signals from GABAergic neurons that counteract the excitatory effect of acetylcholine, delaying paralysis. As a result, the percentage of paralyzed worms over time serves as an indicator of the E/I ratio at the NMJ. When young-adult hermaphrodite and male worms were exposed to aldicarb, nearly all the males were paralyzed within 60 min. In contrast, no paralysis was observed in hermaphrodites (Fig. 1 F). These findings clearly suggested that males are more sensitive to aldicarb and suggest a higher E/I ratio at NMJs in males.

To study the temporal development of sexually dimorphic synaptic transmission at NMJs, we analyzed the E/I ratio in hermaphrodites and males at different developmental stages (L3, L4, and young adults) by aldicarb sensitivity assay. We observed no differences in aldicarb sensitivity between the L3-staged hermaphrodites and males (Fig. S1, A and B). In contrast, the L4-staged males presented significantly increased sensitivity to aldicarb than hermaphrodites (Fig. S1 C), and these sex differences became more pronounced in adults (Fig. S1 D), suggesting that the sexually dimorphic synaptic transmission at NMJs emerges at the L4 stage. This finding aligns with the known timeline of sexual maturation in the male nervous system (Lawson et al., 2019; Pereira et al., 2019).

The aforementioned experiments were carried out in the Bristol N2 strain. To study whether this sexually dimorphic synaptic transmission at NMJs exists in other *C. elegans* strains, we measured the NMJ E/I ratio in both sexes across different natural strains, including the Madison strain TR389, Australian strain AB3, and the Hawaiian strain CB4856. Consistently, males exhibited an increased E/I ratio compared with hermaphrodites of the same strain, recapitulating our initial discovery with the N2 strain (Fig. S1, E–G).

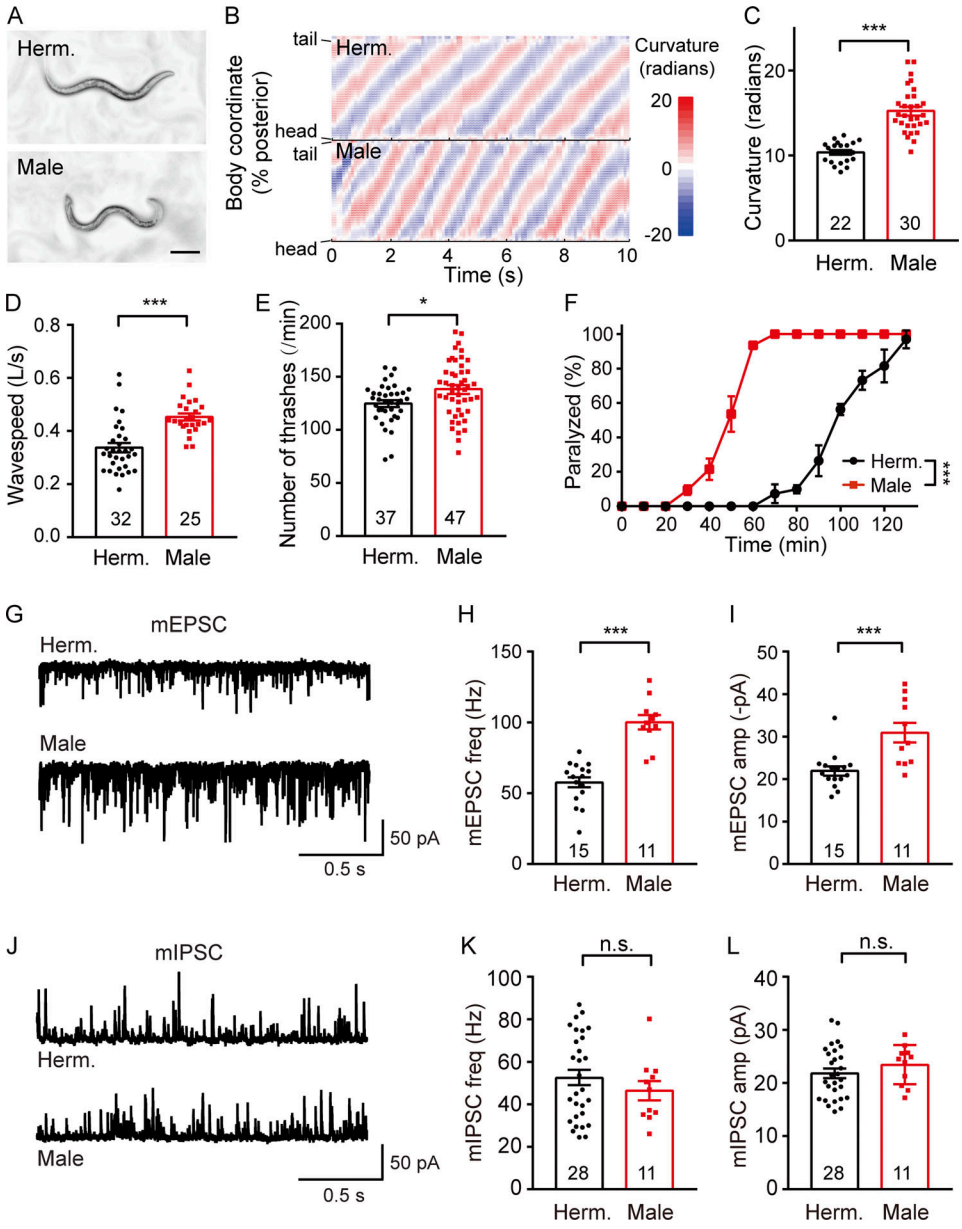

Figure 1. **Cholinergic synaptic transmission is significantly higher in males than in hermaphrodites. (A)** Representative images of body posture during sinusoidal movement in hermaphrodites (Herm.) and males. Scale bar, 150 µm. **(B)** Color plot showing the waves of curvature propagating along the body of a representative hermaphrodite (Herm., top) and a male (Male, bottom). **(C)** Scatter plot showing the body-bend curvature in hermaphrodites (Herm.) and males (Male). **(D)** Locomotion behavior analysis of a single adult hermaphrodite (Herm.) and a male (Male). The averaged and individual crawling locomotion velocities were plotted. **(E)** Body bends (Thrashes) in the liquid culture of hermaphrodites (Herm.) and males (Male). **(F)** Time course analysis of 1.4 mM aldicarb-induced paralysis in hermaphrodites (Herm.) and males (Male). **(G–I)** Endogenous acetylcholine transmission was assessed by recording mEPSCs from body-wall muscles of wild-type adult hermaphrodites (Herm.) and males (Male). Representative mEPSC traces (G), the mean mEPSC frequencies (H), and the mean mEPSC amplitudes (I) are shown. **(J–L)** Endogenous GABA transmission was assessed by recording mIPSCs from body-wall muscles of wild-type adult hermaphrodites (Herm.) and males (Male). Representative mIPSC traces (J), the mean mIPSC frequency (K), and the mean mIPSC amplitude (L) are shown. In C–E, H, I, K, and L, data are presented as mean values ± SEM. Ns represent the number of animals tested. Two-tailed and unpaired Student's *t* test. In F, for each of the group, $n = 3$ biologically independent samples; each sample contains ≥25 animals. Data are presented as mean values ± SEM. Two-way ANOVA comparing all of the time points. *P < 0.05, ***P < 0.001, n.s. not significant.

The higher NMJ E/I ratio in males results from elevated cholinergic transmission

Definitionally, the observed increased NMJ E/I ratio could be caused by increased cholinergic transmission or by decreased GABAergic transmission. To distinguish between these two possibilities, we analyzed spontaneous miniature excitatory postsynaptic currents (mEPSCs) and miniature inhibitory postsynaptic currents (mIPSCs) at NMJs of the two sexes. We performed patch-clamp recordings on the shared muscle cells VR13 or VR11 and found that the mEPSC frequency was significantly higher in males than in hermaphrodites (Fig. 1, G and H), and the mEPSC amplitude was also significantly increased

in males (Fig. 1, G and I). However, we detected no significant differences in mIPSC frequency or amplitude between hermaphrodites and males (Fig. 1, J–L). It is worth noting that a recent study has reported similar findings, demonstrating enhanced neurotransmission at NMJs in males (Yan et al., 2022). Thus, our electrophysiology results support the notion that the higher NMJ E/I ratio observed in males is primarily due to increased cholinergic transmission rather than decreased GABAergic transmission.

The sexually dimorphic cholinergic transmission at NMJs may not be mediated by postsynaptic receptors

The increased cholinergic transmission in males could result from either more abundant postsynaptic receptors or from a higher frequency of presynaptic acetylcholine release. To study which of these processes mediate the sexually dimorphic cholinergic transmission, we examined the effect of two types of nicotinic acetylcholine receptors (UNC-29 and ACR-16; Richmond and Jorgensen, 1999). We used aldicarb sensitivity assays to assess cholinergic transmission at NMJs in *acr-16* and *unc-29* mutant hermaphrodites and males. Though *acr-16* mutant males present slightly but significantly decreased aldicarb sensitivity than wild-type males, they still displayed significantly increased aldicarb sensitivity compared with *acr-16* mutant hermaphrodites (Fig. 2 A). Similarly, a comparison of aldicarb sensitivity between *unc-29* mutant hermaphrodites and males revealed that *unc-29* males were more sensitive to aldicarb than the *unc-29* mutant hermaphrodites, and all *unc-29* mutant animals exhibited resistance to aldicarb (Fig. 2 B). As a result, we recorded mEPSCs at NMJs of *unc-29* mutants. While the increased mEPSC amplitude observed in males compared with hermaphrodites was abolished by *unc-29* mutation, it is worth noting that the mEPSC frequency remained significantly higher in *unc-29* males than in *unc-29* hermaphrodites (Fig. 2, C–E). Collectively, these multiple lines of evidence suggested that the observed sex-differential cholinergic transmission is unlikely to result from the differences in the distribution of postsynaptic receptors between the two sexes, pointing toward a mechanism based on differential presynaptic acetylcholine release.

Males accumulate relatively higher levels of the presynaptic SVs-associated protein UNC-57/endophilin at their cholinergic motor neuron terminals

We next investigated whether presynaptic structures (e.g., SVs) of cholinergic motor neurons differ between hermaphrodites and males. The *C. elegans* NMJs are formed by arms extending from muscle cells toward cholinergic and GABAergic motor neurons. We labeled the cholinergic synapses by genetically fusing GFP to the endogenous UNC-57/Endophilin in cholinergic motor neurons using a split GFP complementation system (Cabantous et al., 2005; Kamiyama et al., 2016). Endophilin is a membrane-associated protein that is required for SVs endocytosis (Ringstad et al., 1999; Schmidt et al., 1999; Schuske et al., 2003). We used CRISPR/Cas9 system to insert a sequence encoding seven GFP11 fragments at the C-terminus of UNC-57/endophilin (Hao et al., 2023). In parallel, the GFP1-10 fragment was constitutively expressed in DA and DB cholinergic motor neurons or GABAergic motor neurons under the control of the *unc-129* or *unc-25* promoters, respectively (Fig. 3 A). DA and DB motor neurons receive synaptic inputs in the ventral nerve cord and form NMJs with the body-wall muscle in the dorsal nerve cord, resulting in the formation of puncta comprising endogenous localized UNC-57 at cholinergic and GABAergic synapses. We observed a significantly higher GFP fluorescence intensity in males compared with hermaphrodites at cholinergic synapses (Fig. 3, B and C). Note that there were no differences in signal density between the two sexes (Fig. 3, B and D). The increased GFP fluorescence in males is unlikely to be attributed to the sex-differential expression of GFP 1–10. We observed no significant differences in puncta fluorescence intensities and densities of the GFP-RAB-3 fusion protein, driven by the *unc-129* promoter, between hermaphrodites and males (Fig. S2, A–C). Further, GABAergic synapses showed no differences between the sexes in UNC-57-GFP fusion fluorescence intensity (Fig. 3, E–G). Thus, the known SV-associated protein UNC-57 is enriched at cholinergic motor neuron terminals in males, suggesting that SVs may differ between the two sexes.

Male cholinergic motor neuron terminals are enriched for synaptic vesicles (SVs)

To study the abundance and distributions of SVs at cholinergic motor neuron terminals, we employed scanning electron microscopy (SEM) to study the ultrastructural organization of cholinergic synapses at NMJs. Hermaphrodite and male worms were subjected to high-pressure freezing (HPF), followed by freeze substitution (FS), 50 nm serial section, and 3D reconstruction by AMIRA software (Siksou et al., 2007; Stigloher et al., 2011). The NMJ synapses were identified based on a set of serial sections (each containing a 50 nm synaptic profile) that meet the following criteria: (i) presence of a presynaptic specialization known as a dense projection (DP) adjacent to a muscle membrane; (ii) two flanking sections from both sides lacking a presynaptic specialization; (iii) presence of synaptic vesicles characterized as spherical, light-tray structures with an average diameter of ∼30 nm (Fig. 4, A and C; and Fig. S2, D and E). We focused on regions within the ventral or dorsal nerve cord, which house cholinergic and GABAergic motor neurons distinguishable by their anatomical features (Markert et al., 2020; White et al., 1986; Xuan et al., 2017; Yu et al., 2018; Fig. S2 F).

We compared the SVs at the cholinergic synapses between the two sexes and found that the total number of SVs within a 50 nm synaptic profile area of 253,900 nm^2 was significantly higher in males compared with hermaphrodites (averaging 40.2 SVs in males vs. 24.2 in hermaphrodites; Fig. 4, A and B). Further, the number of dense core vesicles (DCVs) that are required for transporting neuropeptides and other neurotrophic factors was also significantly higher in males (Fig. 4, A and B). We also compared the docked synaptic vesicles (DSVs; defined as vesicles 0 nm separation from the plasma membrane) and the area of synaptic profile in cholinergic motor neuron terminals in the two sexes: no differences were evident between hermaphrodites and males (Fig. 4, A and B). Finally, we also examined the SVs, DCVs, DSVs, and synaptic profile areas at GABAergic synapses, and they were all comparable between the two sexes (Fig. 4, C

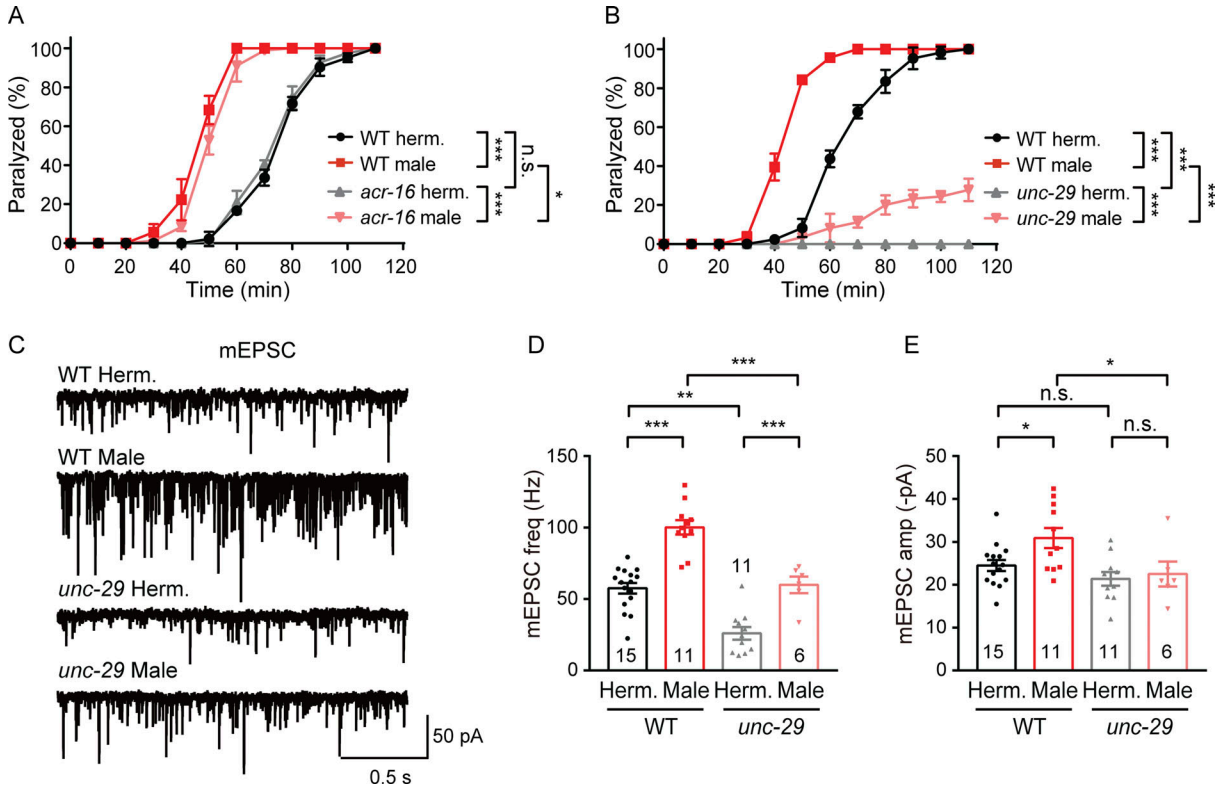

Figure 2. **The sexually dimorphic cholinergic transmission is not likely mediated by postsynaptic acetylcholine receptors. (A and B)** Time course analysis of 1.4 mM aldicarb-induced paralysis in *acr-16* (A) and *unc-29* (B) mutant hermaphrodites (Herm.) and males (Male). **(C–E)** Endogenous acetylcholine transmission was assessed by recording mEPSCs from body-wall muscles of wild-type and *unc-29* mutant adult hermaphrodites (Herm.) and males (Male). Representative mEPSC traces (C), the mean mEPSC frequencies (D), and the mean mEPSC amplitudes (E) are shown. The data for WT are the same as in Fig. 1, H and I. In A and B, for each group, n = 3 biologically independent samples; each sample contains ≥25 animals. Data are presented as mean values ± SEM. Two-way ANOVA comparing all of the time points. In D and E, data are presented as mean values ± SEM. Ns represent the number of animals tested. One-way ANOVA with post-hoc Bonferroni's multiple comparisons. *P < 0.05, **P < 0.01, ***P < 0.001, n.s. not significant.

and D). Collectively, our data showed that males possess more abundant SVs in their cholinergic motor neuron terminals, which is very likely contributing to the sexually dimorphic cholinergic synaptic transmission.

UNC-43/CaMKII is an essential component for the sexually dimorphic abundance of SVs and DCVs in cholinergic synapses

To study the molecular mechanism underlying the sexually dimorphic abundance of SV and DSV at the cholinergic synapses, we analyzed transcriptomic databases at various developmental stages in the two sexes (Kim et al., 2016) and searched for genes that are expressed in cholinergic motor neurons (Taylor et al., 2021) and are specifically upregulated in males during the L4 stage when the sexually dimorphic cholinergic transmission at NMJs emerges. We identified 1,176 genes that are enriched in males specifically at L4 and adult stages, but not in the L3 stage. Among these genes, 208 were expressed in the DA, DB, VA, and VB cholinergic motor neurons (Fig. S3, A and B). Here, we focused our attention on UNC-43/CaMKII since it plays important roles in synaptic transmission and regulates the abundance of DCVs and SVs (Hao et al., 2023; Hoover et al., 2014; Liu et al., 2007).

CaMKII is a serine/threonine-specific protein kinase activated by Ca^{2+}/calmodulin and is required for synaptic transmission and plasticity at both pre- and postsynapses (Hao et al., 2023; Lisman et al., 2002; Sheng and Hoogenraad, 2007). Previous studies have indicated that presynaptic CaMKII is required for the biogenesis of SVs and DCVs and for the synaptic transmission at *Drosophila* and *C. elegans* NMJs (Carrillo et al., 2010; Hoover et al., 2014; Liu et al., 2007). We first verified the sex-differential expression of UNC-43/CaMKII at cholinergic synapses in NMJs during various developmental stages. We examined the localization of endogenous UNC-43/CaMKII at cholinergic synapses by split GFP complementation system and observed a punctate pattern along the nerve cord (Fig. 5, A and B; Hao et al., 2023). We observed a dramatic increase in puncta fluorescence intensities in L4-staged and adult males compared with their respective hermaphrodites (Fig. 5, B and C), while no significant differences were observed between L3-staged males and hermaphrodites (Fig. 5, B and C). There were no differences in puncta densities between the two sexes at all stages examined (Fig. 5, B and D). In parallel, we examined the expression and localization of UNC-43 at GABAergic synapses and found that no differences were observed between the two sexes (Fig. 5, E–G). These findings support the transcriptome data analysis, indicating that the sex-specific expression of UNC-43 in cholinergic motor neurons at the NMJs emerges after the L4 stage.

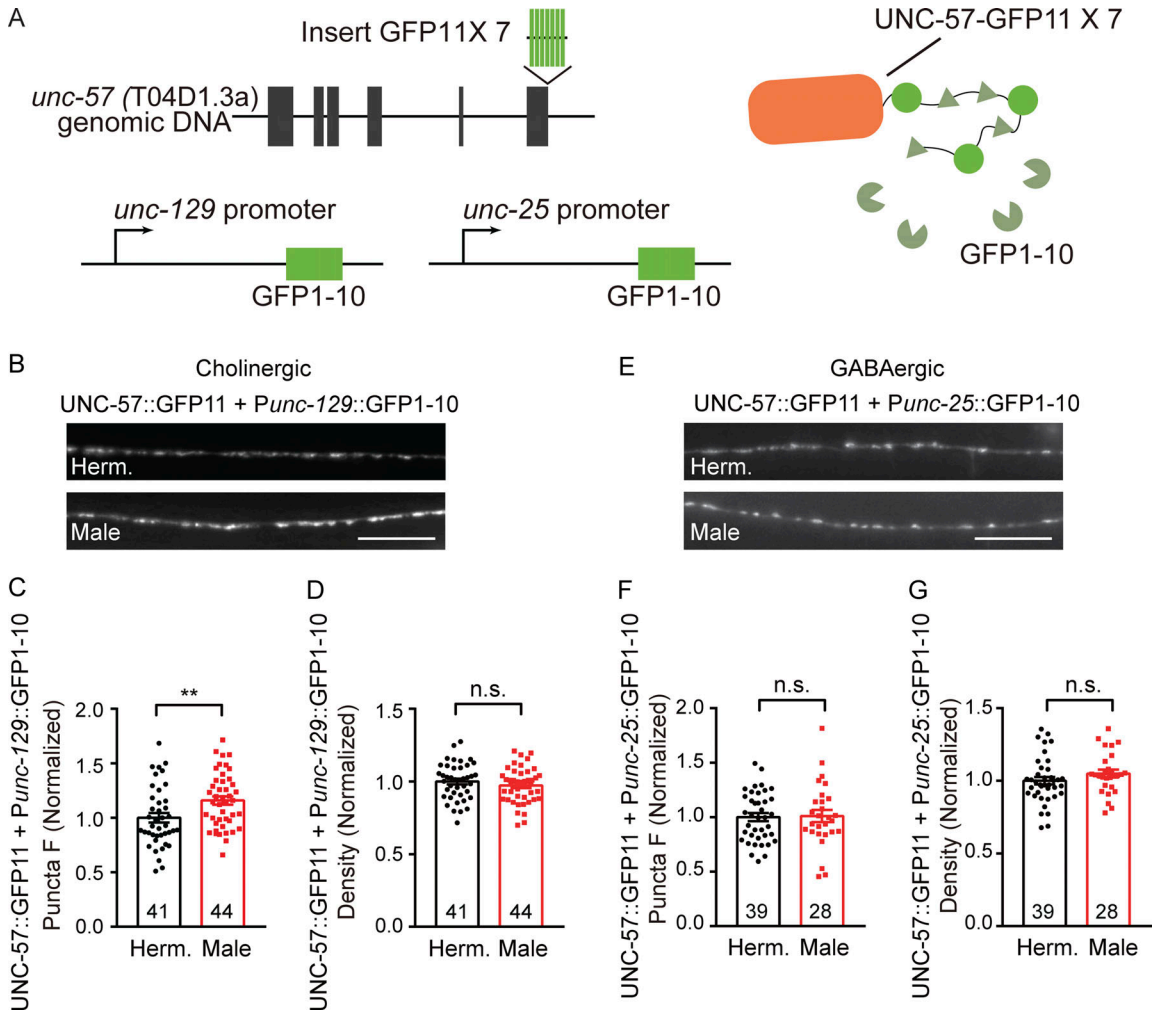

Figure 3. **UNC-57/Endophilin is enriched in males at their cholinergic motor neuron terminals. (A)** Schematic illustration of split GFP complementation experimental design. Seven copies of the split GFP11 were inserted into the C-terminal of *unc-57* (T04D1.3a) genomic loci by CRISPR-Cas9 system. The split GFP1-10 was expressed in the B-type cholinergic and GABAergic motor neurons by *unc-129* and *unc-25* promoters, respectively. **(B–D)** The puncta fluorescence intensities and densities, marked by the cholinergic synaptic UNC-57::split GFP in dorsal nerve cord axons in hermaphrodites (Herm.) and males (Male). Representative images (B), mean puncta intensity (C), and density (D) are shown. **(E–G)** The puncta fluorescence intensities and densities, marked by the GABAergic synaptic UNC-57::split GFP in dorsal nerve cord axons in hermaphrodites (Herm.) and males (Male). Representative images (E), mean puncta intensity (F), and density (G) are shown. In B and E, Scale bars, 10 µm. In C, D, F, and G, data are presented as mean values ± SEM. Ns represent the number of animals tested. Two-tailed and unpaired Student's *t* test. **P < 0.01, n.s. not significant.

To study if the sex-differential expression of UNC-43 contributes to the sexually dimorphic SVs and DCVs in cholinergic motor neuron terminals, we examined the ultrastructure of cholinergic synapses using SEM in *unc-43* knockout hermaphrodites and males. Our data revealed that both *unc-43* mutant hermaphrodites and males exhibited a significant reduction in the number of DCVs compared with their respective wild-type worms (Fig. 6, A–C), which is consistent with a previous report (Hoover et al., 2014). Notably, *unc-43* mutant males, but not *unc-43* mutant hermaphrodites, displayed a significant decrease in the number of SVs compared with wild-type males, whereas no significant differences in SV or DCV numbers were observed between hermaphrodites and males in the *unc-43* mutant animals (Fig. 6, A–C). These results indicate that UNC-43 is required for the sexually dimorphic abundance of SVs and DCVs at cholinergic synapses.

UNC-43/CaMKII is required for sexually dimorphic cholinergic synaptic transmission and locomotion behaviors

To study if the sex-differential abundance of SVs mediated by UNC-43/CaMKII contributes to sexually dimorphic cholinergic synaptic transmission, we performed patch-clamp recordings of mEPSCs in body-wall muscles of both *unc-43* knockout mutant hermaphrodites and males. Consistent with the previous report, mEPSC frequencies and amplitudes were dramatically decreased in *unc-43* mutants compared with the wild type for both hermaphrodites and males (Fig. 6, D–F), supporting that UNC-43 is required for synaptic neurotransmission. Further, we noted that the magnitude of the increase in mEPSC frequency and amplitude in males over hermaphrodites was blocked in *unc-43* mutants as compared with the wild type (Fig. 6, D–F). These findings provide further support that UNC-43 is required for sexually dimorphic cholinergic synaptic transmission at NMJs.

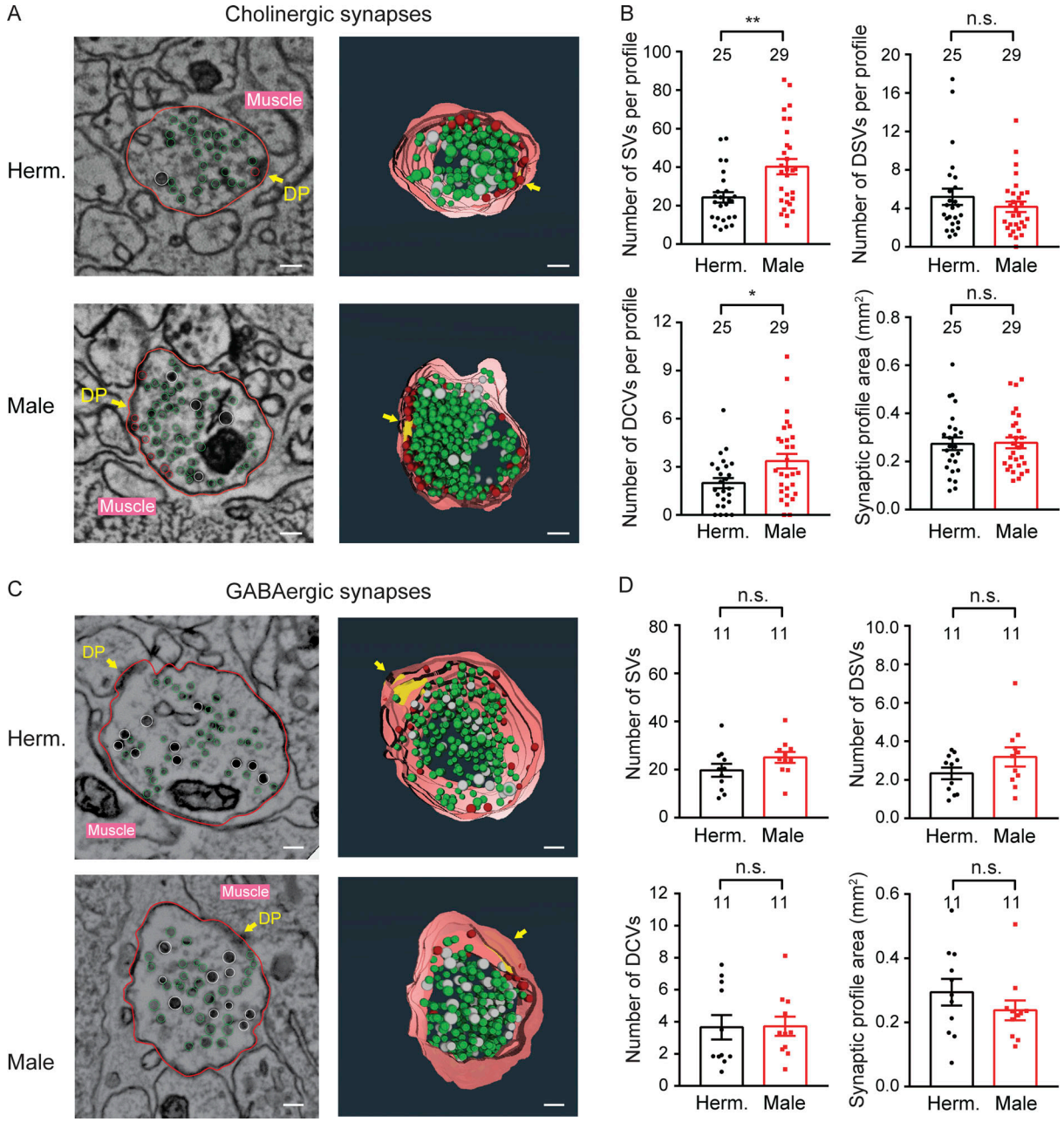

Figure 4. **Males accumulate relatively more SVs and DCVs at their cholinergic motor neuron terminals. (A and C)** Representative micrographs and 3D reconstruction of cholinergic synaptic profiles (A) and GABAergic synaptic profile (C) in hermaphrodites (Herm.) and males (Male). Yellow arrows indicate the dense projection (DP). In the 3D reconstruction, the synaptic vesicles (SVs) are marked as green, the docked synaptic vesicles (DSVs) are marked as red, the dense core vesicles (DCVs) are marked as white, and the DP is marked as yellow. Scale bar, 200 nm. **(B and D)** The number of cholinergic total SVs, DSVs, and DCVs in a 50 nm cholinergic synaptic profile (B) and GABAergic synaptic profile (D) as well as the synaptic profile area are measured in hermaphrodites (Herm.) and males. In B and D, data are presented as mean values ± SEM. Ns represent the number of synapses analyzed. Two-tailed and unpaired Student's *t* test. *P < 0.05, **P < 0.01, n.s. not significant.

Importantly, we have ruled out the possibility that there is a basal requirement of synaptic vesicle release for the observed sexually dimorphic cholinergic transmission. In *rab-3* mutants, where synaptic vesicle release is dramatically impaired, we still observed a significant increase in mEPSC frequency in *rab-3* males compared with *rab-3* hermaphrodites (Fig. S3, C–E), supporting the conclusion that UNC-43 is specifically required for the sexually dimorphic cholinergic transmission.

We next studied whether UNC-43 also is required for sexually dimorphic locomotion behaviors by comparing the locomotor ability of *unc-43* mutant hermaphrodites and males. In both sexes, we observed a significant decrease in sinusoidal movement velocity, body curvature, and thrashing frequency in *unc-43* mutants compared with the wild type (Fig. 6, G–I). Importantly, the sexual dimorphism observed in all locomotion behaviors was abolished in *unc-43* mutants (Fig. 6, G–I). Collectively,

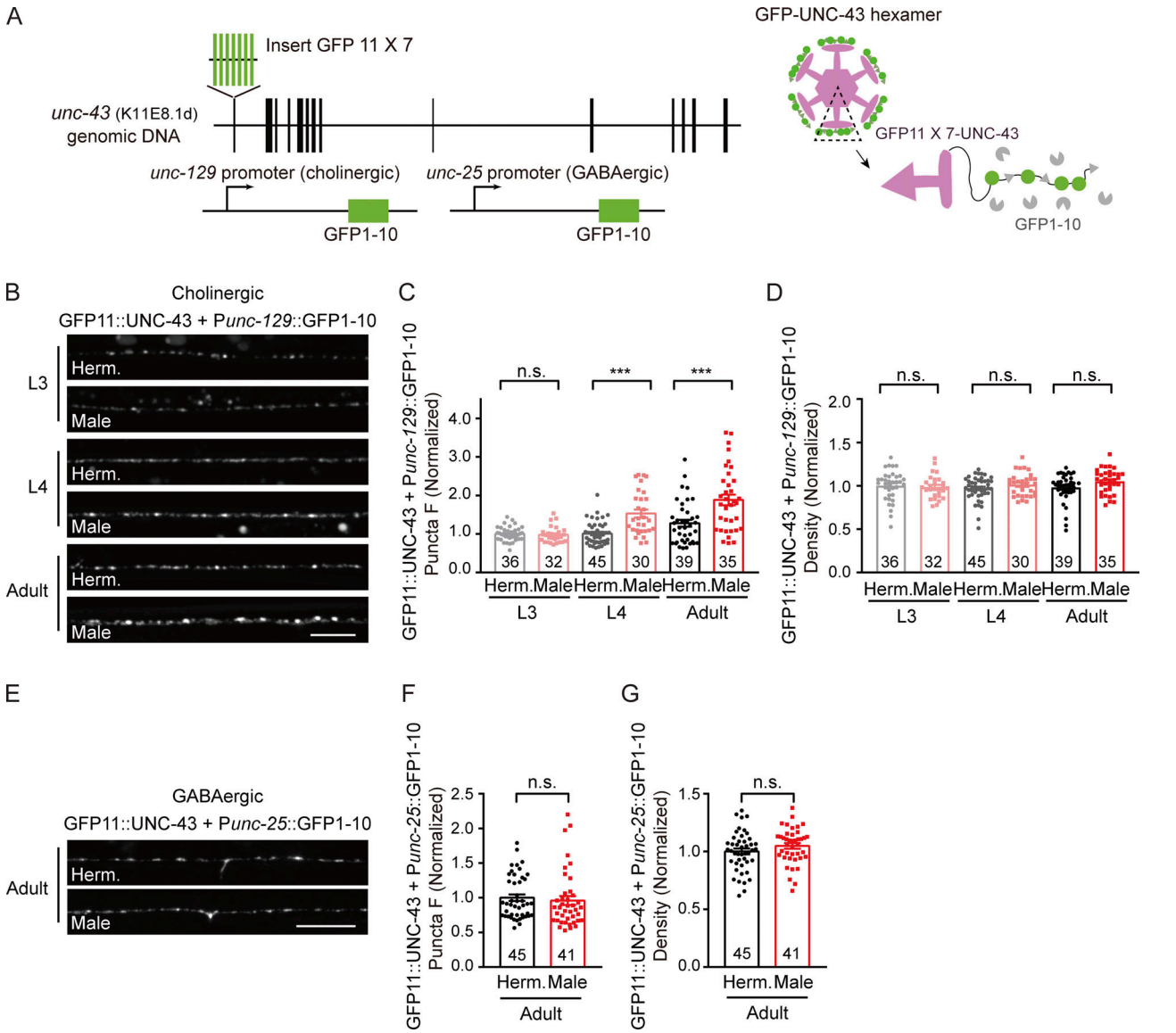

Figure 5. **UNC-43 is enriched in males at the cholinergic motor neuron terminals. (A)** Schematic illustration of split GFP complementation experimental design. Seven copies of the split GFP11 were inserted into the N-terminal of *unc-43* (K11E8.1d) genomic loci by CRISPR-Cas9 system. The split GFP1-10 was expressed in B-type cholinergic and GABAergic motor neurons by *unc-129* and *unc-25* promoters, respectively. **(B–D)** The puncta fluorescence intensities and densities, marked by the cholinergic synaptic UNC-43::split GFP in dorsal nerve cord axons in the L3-staged, L4-staged, and adult hermaphrodites (Herm.) and males (Male). Representative images (B), mean puncta intensity (C), and density (D) are shown. **(E–G)** The puncta fluorescence intensities and densities, marked by the GABAergic synaptic UNC-43::split GFP in dorsal nerve cord axons in the adult hermaphrodites (Herm.) and males (Male). Representative images (E), mean puncta intensity (F), and density (G) are shown. In B and E, Scale bars, 10 µm. In C, D, F, and G, data are presented as mean values ± SEM. Ns represent the number of animals tested. One-way ANOVA with post-hoc Bonferroni's multiple comparisons for C and D and two-tailed and unpaired Student's *t* test for F and G. ***P < 0.001, n.s. not significant.

these data support that the UNC-43 is required for sexually dimorphic animal locomotion behaviors.

To investigate whether UNC-43 functions at cholinergic motor neurons to regulate sexually dimorphic synaptic transmission, we generated worms with conditional deletion of *unc-43* in (i) cholinergic motor neurons, (ii) GABAergic motor neurons, or (iii) muscle cells (Fig. 7 A; Hao et al., 2023). We found that the deletion of *unc-43* specifically in cholinergic motor neurons replicates the phenotype observed in *unc-43* knockout mutants, showing a significant decrease in mEPSC frequency (Fig. 7, B–D). Note that no apparent defects in mEPSC frequency or amplitude were observed in the strains with *unc-43* deletion in GABAergic motor neurons or muscle cells (Fig. 7, B–D). Additionally, we observed that the sexual dimorphism in sinusoidal locomotion velocity was abolished in worms with *unc-43* deletion specifically in cholinergic neurons (Fig. 7 E), while no such effect was observed in worms with *unc-43* deletion in GABAergic neurons or muscle cells (Fig. 7, F and G). These lines of evidence demonstrate that UNC-43 functions specifically at cholinergic motor neurons to support cholinergic synaptic transmission and mediate sexually dimorphic locomotion behaviors.

Considering the high abundance of presynaptic UNC-43 at cholinergic synapses in males, we then investigated whether a

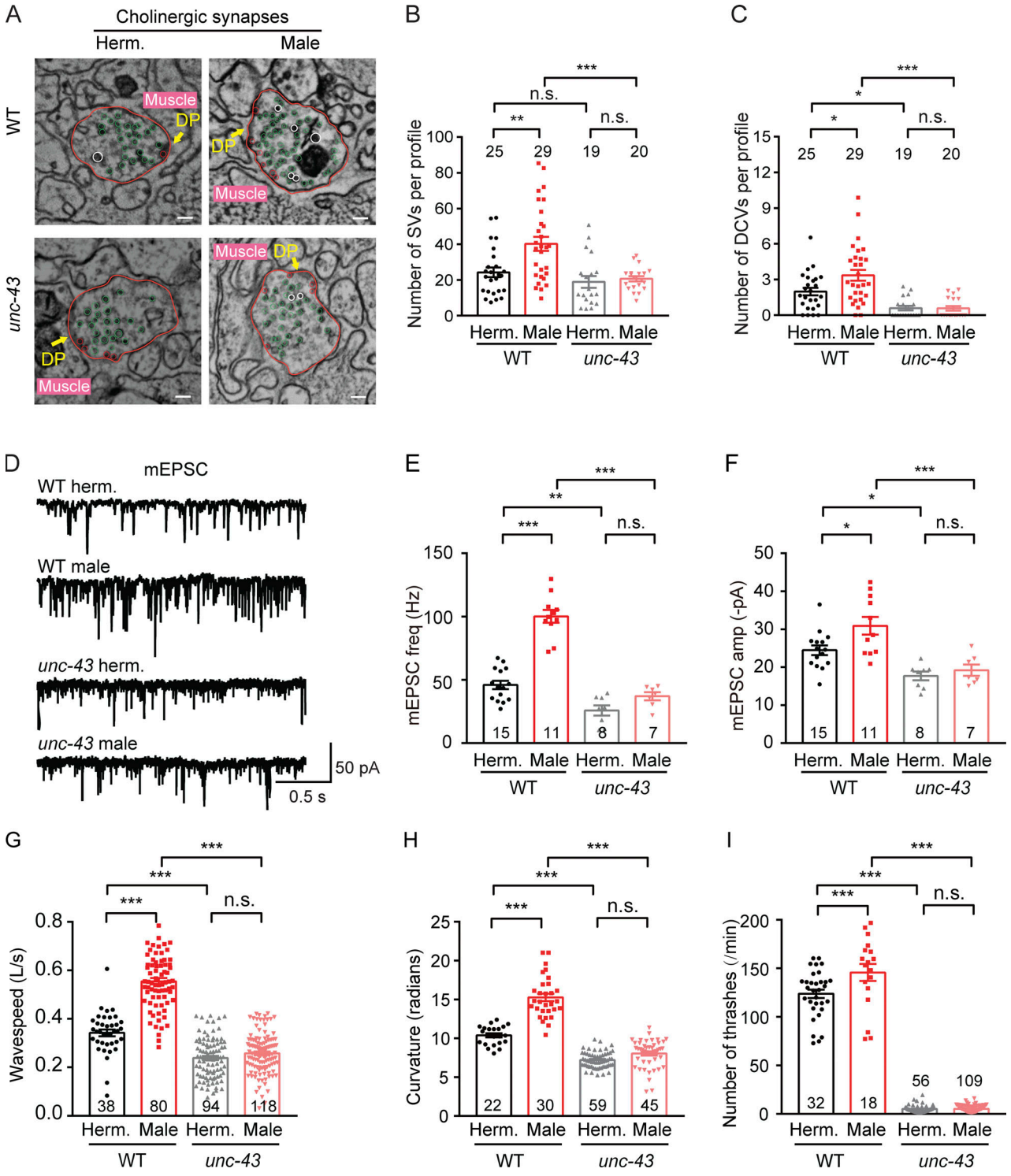

Figure 6. **UNC-43 is required for the sexually dimorphic SVs abundance and cholinergic transmission. (A–C)** Ultrastructural analysis of cholinergic SVs and DCVs in *unc-43* mutant hermaphrodites (Herm.) and males (Male). **(A)** Representative micrographs of cholinergic synaptic profiles in *unc-43* mutant hermaphrodites (Herm.) and males. The synaptic vesicles (SVs) are marked as green, the docked synaptic vesicles (DSVs) are marked as red, the dense core vesicles (DCVs) are marked as white, and the DP is marked as yellow. Scale bar, 200 nm. The number of total SVs (B) and DCVs (C) in 50-nm synaptic profile in hermaphrodites (Herm.) and males were measured in wild type (WT) and *unc-43* mutants. The data used for the analysis of wild-type hermaphrodites and males is the same as presented in Fig. 4, A and B. **(D–F)** Endogenous acetylcholine transmission was assessed by recording mEPSCs from body-wall muscles of wild-type and *unc-43* mutant adult hermaphrodites (Herm.) and males (Male). Representative mEPSC traces (D), the mean mEPSC frequencies (E), and the mean mEPSC amplitudes (F) are shown. The data for WT are the same as in Fig. 1, H and I. **(G)** Locomotion behavior analysis of *unc-43* mutant hermaphrodites (Herm.) and males (Male). The averaged and individual crawling locomotion velocities were plotted. **(H)** Scatter plot showing the body-bend curvature in *unc-43* mutant hermaphrodites (Herm.) and males (Male). **(I)** Body bends (Thrashes) in the liquid culture of *unc-43* mutant hermaphrodites (Herm.) and males (Male). In B, C, and E–I, data are presented as mean values ± SEM. Ns represent the number of synapses analyzed for B and C and animals tested for E–I. One-way ANOVA with post-hoc Bonferroni's multiple comparisons. *P < 0.05, **P < 0.01, ***P < 0.001, n.s. not significant.

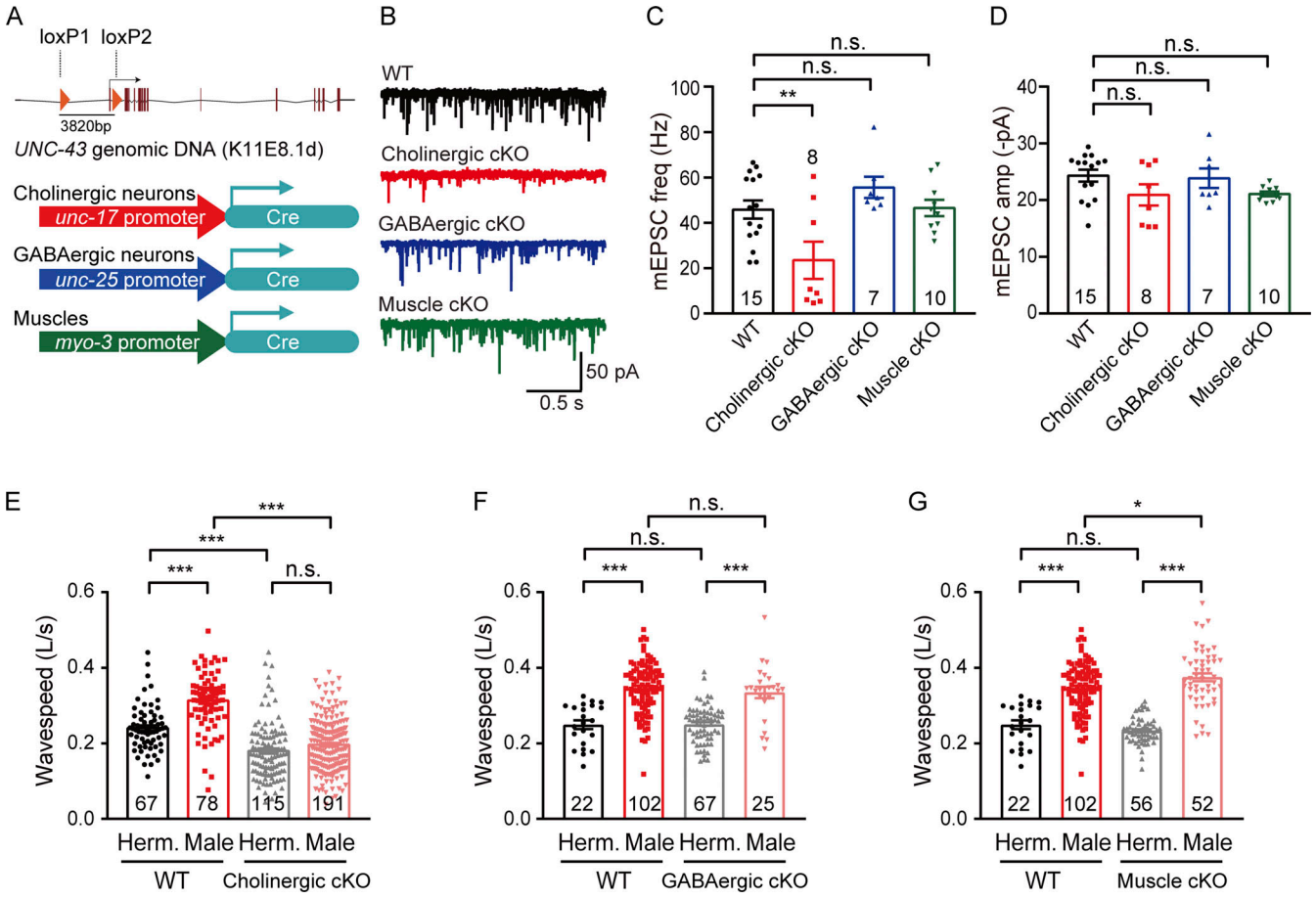

Figure 7. **UNC-43 functions at cholinergic motor neurons to support cholinergic synaptic transmission and sexually dimorphic locomotion behaviors. (A)** Schematic for construction of the *unc-43* conditional deletion lines. Two loxP sites were inserted into the genomic loci at the promoter and the first intron of *unc-43* (K11E8.1d and K11E8.1g) coding sequence using CRISPR/Cas9, the minigene encoding Cre recombinase under *unc-17*, *unc-25*, and *myo-3* promoters were used to knockout *unc-43* gene in cholinergic motor neurons, GABAergic motor neurons, and muscle cells, respectively. **(B–D)** Endogenous acetylcholine transmission was assessed by recording mEPSCs from body-wall muscles of *unc-43* conditional knockout hermaphrodites. Representative mEPSC traces (B), the mean mEPSC frequency (C), and the mean mEPSC amplitudes (D) are shown. **(E–G)** Locomotion behavior analysis of *unc-43* conditional knockout hermaphrodites and males. The averaged and individual crawling locomotion velocities were plotted. The data used for the analysis of wild-type hermaphrodites and males in G are the same as presented in F. In C–G, data are presented as mean values ± SEM. Ns represent the number of animals tested. One-way ANOVA with post-hoc Dunnett multiple comparisons for C and D, one-way ANOVA with post-hoc Bonferroni's multiple comparisons for E–G. *P < 0.05, **P < 0.01, ***P < 0.001, n.s. not significant.

partial knockdown of UNC-43 expression in males would lead to a reduction in cholinergic transmission similar to that observed in hermaphrodites. To achieve this, we employed RNA interference (RNAi) to partially knock down UNC-43 expression in males and found a significant decrease in both the frequency and amplitude of mEPSCs (Fig. S3, F–H). Moreover, we observed a significant reduction in locomotion velocity (Fig. S3 I). In summary, these results demonstrate that the abundance of UNC-43 is involved in maintaining cholinergic transmission and locomotion behavior in males and lend more support to the conclusion that the sex-differential abundance of UNC-43 mediates the sexually dimorphic cholinergic transmission.

The sexually dimorphic cholinergic transmission at NMJs is controlled non-cell-autonomously

Next, we investigated whether sex-specific factors are involved in generating sexually dimorphic cholinergic transmission at NMJs. We screened the effects of multiple factors using aldicarb sensitivity assays, including pheromones (using *daf-22* mutants), hormones (using *daf-12* mutants), gonadogenesis (using *gon-2* mutants), spermatogenesis (using *fog-2* and *fer-6* mutants), germline proliferation (using *glp-1* mutants), and reproduction (FUdR treatment; Fig. S4 A). There was significantly higher aldicarb sensitivity in males compared with their corresponding hermaphrodites for all of these mutant strains or treatment conditions (Fig. S4, B–H), excluding these sex-specific factors from the observed increased cholinergic transmission in males.

Further, we studied whether the increased cholinergic transmission in males could be attributed to sex-specific cholinergic neurons. In males, there are nine male-specific cholinergic motor neurons in the ventral nerve cord (CA1–9), and it is known that the acetylcholine level is relatively low in CA7–9 (Cook et al., 2019). Hermaphrodites, on the other hand, have six sex-specific cholinergic motor neurons (VC1–6). A previous

study showed that the proliferation of both CA1–6 and VC1–6 neurons requires the homeobox gene *lin-39* (Kalis et al., 2014). When we examined *lin-39* mutants (that lack both CA1–6 and VC1–6 neurons), we observed a significantly higher mEPSC frequency in *lin-39* mutant males than in *lin-39* mutant hermaphrodites (Fig. S4, I and J), supporting that the increased cholinergic synaptic transmission in males is not caused by male-specific CA neurons.

Having excluded several sex-specific factors and sex-specific cholinergic neurons, we next investigated whether the sexually dimorphic cholinergic transmission at NMJs is controlled cell autonomously or if it depends on other neurons and/or circuits. For this purpose, we adopted a sex-reversal experimental approach in which we altered the sex of all neurons ("pan-neuron"), cholinergic motor neurons, or GABAergic motor neurons by manipulating the activity of the Gli transcription factor TRA-1, which is a known master regulator of sexual differentiation (Hodgkin, 1987; Hunter and Wood, 1990; Zarkower and Hodgkin, 1992). TRA-1 is expressed in all hermaphrodite cells and promotes hermaphroditic cellular identities and represses male identities (Hunter and Wood, 1990). In males, TRA-1 is degraded, while in hermaphrodites, the degradation of TRA-1 is suppressed by TRA-2 (Mehra et al., 1999; Schvarzstein and Spence, 2006; Starostina et al., 2007; Fig. S5 A), so deletion of *tra-2* can lead to TRA-1 degradation and male cellular identities.

We masculinized neurons in hermaphrodites by neuron-type-specific knockout of the *tra-2* gene. Briefly, we inserted a loxP site at the 20th intron and another site in the downstream 3′UTR of *tra-2* and drove CRE recombinase expression to delete the sequence encoding TRA-2 in cholinergic motor neurons (under the *unc-4* promoter or *unc-17* promoter), GABAergic motor neurons (under the *unc-25* promoter), or pan-neurons (under the *rgef-1* promoter; Kage-Nakadai et al., 2014; Fig. 8 A). The neuron-type specific knockout of TRA-2 was confirmed by examining the expression of TRA-1, which was degraded in neurons with *tra-2* deletion (Fig. S5, A–D). We found that masculinization of neither cholinergic motor neurons nor GABAergic motor neurons in hermaphrodites resulted in increased aldicarb sensitivity or locomotion velocity (Fig. 8, B and C; and Fig. S5 E). However, pan-neuronal masculinization in hermaphrodites did result in a male-like hypersensitivity to aldicarb and higher locomotion velocity (Fig. 8, B and C). We also recorded mEPSCs in the sex-reversal animals and noticed that the mEPSC frequency and amplitude were both significantly increased in hermaphrodites with pan-neuronal masculinization as compared with the wild-type hermaphrodites (Fig. 8, D and E). Notably, there were no significant differences in mEPSC frequency or amplitude between pan-neuronal masculinized hermaphrodites and wild-type males (Fig. 8, D and E).

We further validated our findings by overexpressing TRA-2ic or TRA-1 repressor FEM-3 to feminize males and masculinize hermaphrodites, respectively (Mowrey et al., 2014). By driving FEM-3 expression under corresponding promoters, we masculinized cholinergic neurons, GABAergic neurons, and pan-neurons in hermaphrodites, and examined synaptic transmission by an aldicarb sensitivity assay. We found that masculinization of cholinergic neurons resulted in a modest increase in aldicarb sensitivity in hermaphrodites, while masculinization of GABAergic neurons had no significant effect (Fig. S5 F). Notably, hermaphrodites with pan-neuronal masculinization exhibited a dramatic increase in aldicarb sensitivity (Fig. S5 F). Additionally, we feminized specific neurons in males by overexpressing the intracellular domain of TRA-2 (TRA-2ic). The pan-neuronal feminization led to a decrease in aldicarb sensitivity, while the feminization of cholinergic neurons and GABAergic neurons did not have a significant impact (Fig. S5 G). These sex-reversal experiments support a non-cell-autonomous control mechanism underlying the sexually dimorphic cholinergic transmission and suggest that additional sex-specific circuitry is required to regulate the observed male-specific increase in cholinergic transmission at NMJs.

Recall that our experiments showed a higher abundance of UNC-43 at cholinergic synapses in males compared with hermaphrodites, which contributes to sexually dimorphic cholinergic transmission and locomotion behaviors. Building upon these findings, we further investigated whether the sex-reversal of all neurons in hermaphrodites would lead to a male-like increase of presynaptic UNC-43/CaMKII (Fig. 5, B and C). Our findings revealed that hermaphrodites with pan-neuronal masculinization, but not those with cholinergic neurons masculinization, exhibited a significant increase in the presynaptic abundance of UNC-43 at cholinergic synapses (Fig. 8 F), supporting the notion that sex-specific circuitry regulates the abundance of presynaptic UNC-43 to generate the sex-dependent cholinergic transmission at NMJs.

Discussion

In this study, we have revealed previously unknown sexually dimorphic synaptic transmission at NMJs that mediates the sex-specific locomotion behaviors in *C. elegans*. We have shown that the frequency of cholinergic synaptic transmission is significantly higher in males than in hermaphrodites. We found that sexually dimorphic cholinergic transmission is not mediated by the cholinergic receptors. Through our SEM analysis, we revealed that males possess significantly more SVs and DCVs at their cholinergic synapses, which requires UNC-43/CaMKII that present sex differential expression in the cholinergic neurons. Considering the roles of SVs in synaptic transmission, the high abundance of SVs at the cholinergic motor neuron terminals in males likely accounts for the increased cholinergic transmission, which in turn explains the altered locomotion behaviors. Further, we showed that the sex-specific synaptic transmission at cholinergic synapses in NMJs is controlled in a non-cell-autonomous manner and involves additional male-specific neuronal circuitry. Our results provide mechanistic insights into how sex-shared neurons can generate a sex-specific form of synaptic transmission and shed light on the understanding of sexual dimorphism in locomotor behaviors and the prevalence of psychiatric disorders.

Compared with a mammalian nervous system (containing 86 billion neurons in humans and 75 million neurons in mice), *C. elegans* has a much simpler nervous system consisting of only 302 neurons in hermaphrodites and 387 neurons in males,

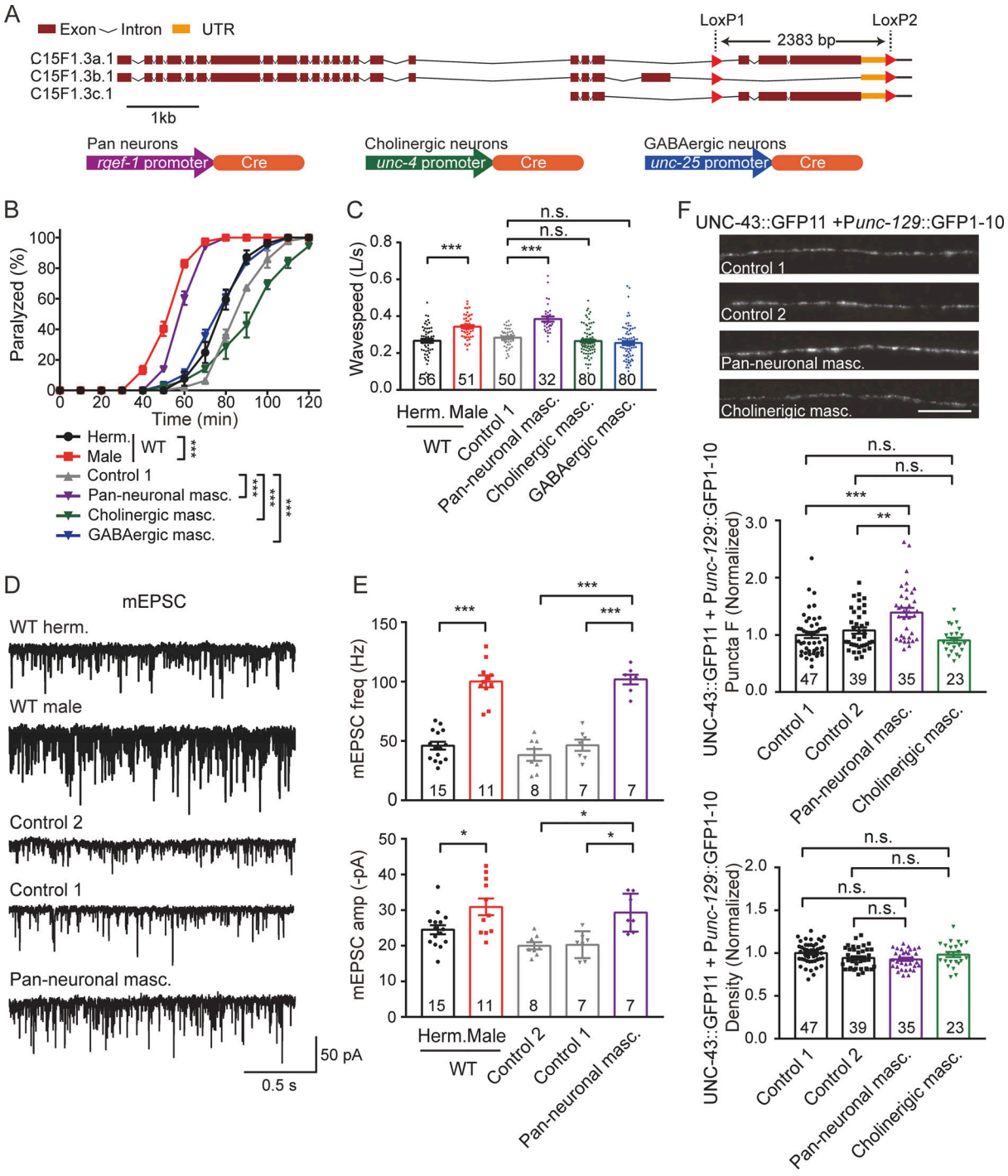

Figure 8. **The sexually dimorphic cholinergic transmission is controlled by the sex identities of the entire nervous system. (A)** Schematic for construction of the *tra-2* (C15F1.3) conditional deletion lines. Two loxP sites were inserted into the 20th intron and the second loxP downstream the 3′ UTR using CRISPR/Cas9, the minigene encoding Cre recombinase under *rgef-1*, *unc-4*, and *unc-25* promoters were used to knock out *tra-2* gene in pan-neurons, cholinergic motor neurons, and GABAergic motor neurons. **(B)** Time course analysis of 1.4 mM aldicarb-induced paralysis in *tra-2* conditional knockout hermaphrodites (Herm.) and males (Male). Knock out *tra-2* gene in all neurons, cholinergic neurons, and GABAergic neurons to get pan-neuronal masculinized (Pan-neuronal masc.), Cholinergic neuronal masculinized (Cholinergic masc.), and GABAergic neuronal masculinized (GABAergic masc.) hermaphrodites. Transgenic animals with two loxP sites insertion but without Cre recombinase expression were used as controls (Control 1). **(C)** Locomotion behavior analysis of a single adult *tra-2* conditional knockout hermaphrodite (Herm.) and a male (Male). The averaged and individual crawling locomotion velocities were plotted. **(D and E)** Endogenous acetylcholine transmission was assessed by recording mEPSCs from body-wall muscles of *tra-2* conditional knockout hermaphrodites. Representative mEPSC traces (D), the mean mEPSC frequencies (E, top panel), and the mean mEPSC amplitudes (E, bottom panel) are shown. Transgenic animals with two loxP sites insertion but without Cre recombinase expression were used as control 1, and transgenic animals with pan-neuronal Cre recombinase expression, but without two loxP sites insertion were used as control 2. The data for WT are the same as in Fig. 1, H and I. **(F)** The puncta fluorescence intensities and densities, marked by the cholinergic synaptic UNC-43::split GFP in dorsal nerve cord axons in *tra-2* conditional knockout

hermaphrodites. Representative images (top panel, scale bar, 10 µm), mean puncta intensity (middle panel, and density (bottom panel) are shown. In B, for each of the group, n = 3 biologically independent samples; each sample contains ≥25 animals. Data are presented as mean values ± SEM. Two-way ANOVA comparing all of the time points. In C, E, and F, data are presented as mean values ± SEM. Ns represent the number of animals tested. One-way ANOVA with post-hoc Bonferroni's multiple comparisons. *P < 0.05, **P < 0.01, ***P < 0.001, n.s. not significant.

including both sex-specific and sex-shared neurons. *C. elegans* serves as an excellent model for identifying sex-specific neuron types and sex-shared neurons with sexually dimorphic functions. Previous studies have identified eight hermaphrodite-specific neurons (including the HSN neuron pair and the six VC neurons) responsible for the egg-laying behavior and 93 male-specific neurons participating in the copulation behaviors. However, sex-shared neurons also play substantial roles in mediating sexually dimorphic behaviors. Among the 294 sex-shared neurons in *C. elegans*, only a small proportion of them have been found to undergo sex-specific differentiation or to mediate sexually dimorphic behaviors (Emmons, 2014; Fagan and Portman, 2014; Wan et al., 2019).

For instance, in the chemosensory neurons AWA, the G protein-coupled receptor (GPCR) SRD-1 is highly expressed in males but undetectable in hermaphrodites, which mediates a sex-specific pheromone perception behavior in males (Wan et al., 2019; Wang and Hobert, 2019). On the other hand, the expression of diacetyl chemoreceptor ODR-10 in AWA neurons is much lower in males compared with hermaphrodites, which reduces food attraction and promotes mate-searching behaviors in males (Ryan et al., 2014). Additionally, the PHB sensory neurons undergo sex-specific pruning, establishing sexually dimorphic connectivity with interneuron and motor neurons (Oren-Suissa et al., 2016; Salzberg et al., 2020). Moreover, research has revealed that the sensory neuron pair PHC differentiates into a densely connected hub sensory neuron/interneuron, enabling the integration of male-specific synaptic inputs (Serrano-Saiz et al., 2017).

Our findings support the conclusion that the cholinergic neurons alone are insufficient to generate the observed male-specific increase in cholinergic transmission at NMJs, indicating the requirement for additional sex-specific circuitry. It has been established that sensory neurons and interneurons can modulate the development and maintenance of NMJs. For instance, our previous studies have demonstrated that the sensory circuitry involving AWB neurons modulates cholinergic transmission at NMJs in a sex-dependent manner (Qian et al., 2021). Further investigations can be undertaken to explore the involvement of these sex-shared but dimorphic sensory neurons and interneurons in generating sexually dimorphic cholinergic transmission at NMJs.

We demonstrate in the present study that cholinergic motor neurons present sexually dimorphic synaptic transmission in *C. elegans*, and we show that this mediates the sex-specific locomotion behaviors. In the mammalian nervous system, most cholinergic neurons exist at NMJs and in subcortical regions of the brain (Houser et al., 1985). Interestingly, there are also differences in locomotion activities between the two sexes in mice: females perform much better in both the active rotation behavior and motor performance tests as compared with males (Ge et al., 2013; McFadyen et al., 2003; O'Leary et al., 2020). These findings suggest that sexually dimorphic synaptic transmission in cholinergic synapses likely exists in mammalian nervous systems.

A recent study has also reported the adult-specific difference in synaptic vesicles and neurotransmission, specifically at cholinergic synapses but not GABAergic synapses, between males and hermaphrodites (Yan et al., 2022). They proposed that T-type calcium channels/CCA-1 play a male-specific role in acetylcholine release at the NMJs in adult animals. In our study, we showed that presynaptic UNC-43 at cholinergic neurons is more abundant in males compared with hermaphrodites, which controls axonal SV abundance and synaptic transmission.

CaMKII is a serine/threonine kinase that is highly conserved in both *C. elegans* and mammals. It localizes to both pre- and postsynapses. At postsynapses, CaMKII is involved in recruiting the AMPA receptors and mediating the early LTP (Lisman et al., 2012). In presynaptic elements, CaMKII controls the synaptic abundance of SVs and DCVs in both *C. elegans* and mammals (Hoover et al., 2014; Liu et al., 2007; Moro et al., 2020) and triggers anterograde signals to recruit $GABA_A$Rs (Hao et al., 2023). CaMKII regulates the number of DSVs and modulates presynaptic plasticity by regulating the size of the readily releasable pool of SVs (Hojjati et al., 2007). The phosphorylation of synapsin I by CaMKII has been reported to mobilize SVs from the reserve pool.

Here, we have observed a significant difference in CaMKII abundance at cholinergic motor neurons between males and hermaphrodites. Consistent with our findings, recent studies also showed that in mice, the CaMKII-α protein level in the hippocampus is significantly higher in males than in females (Tejos-Bravo et al., 2021). There are also reports that the CaMKII-α expression level can be increased by glucocorticoid receptor deletion—but this only occurs in female mice (Tejos-Bravo et al., 2021). Thus, there is sex-biased expression and regulation in mice. These studies, along with our findings, collectively support that CaMKII-α is a molecule with conserved functions involved in sex-specific synaptic transmission.

It bears emphasis that the sex-differential expression of CaMKII at the NMJs that we detected is specific for cholinergic motor neurons. No such expression difference was observed in the GABAergic motor neurons we examine (Fig. 5), suggesting that sex-specific expression in *C. elegans* can be neuron-type specific. Recall that CaMKII-α is expressed in the hippocampus of mice, which consists of a diversity of neuron types including glutamatergic and GABAergic neurons. It's worth extensive studies to investigate CaMKII-α expression in individual neuron types within the two sexes and study animal behaviors related to such neuron types in both genders.

CaMKIIs have been implicated in many neuropsychiatric diseases, including addiction, depression, schizophrenia, and

several neurodegenerative diseases such as Parkinson's disease (Takemoto-Kimura et al., 2017). Interestingly, many of these diseases show a sexually dimorphic prevalence. For example, schizophrenia and Parkinson's disease are more commonly observed in males, while major depression is more prevalent in females. However, the underlying mechanism for such sexually dimorphic prevalence is unclear. The CaMKII-mediated sexually dimorphic synaptic transmission we identified here may help to deepen understanding of the pathophysiology of certain types of neuropsychiatric and neurodegenerative diseases.

Materials and methods

Reagents

The reagents or resources used in this study are detailed in Table S1.

Strains

The strains used in this study are detailed in Table S2.

Plasmids and primers

The plasmids and primers used in this study are detailed in Table S3.

Software and algorithms

The software and algorithms used in this study are detailed in Table S4.

Further information and requests for resources and reagents should be directed to and will be fulfilled by Xia-Jing Tong (tongxj@shanghaitech.edu.cn).

Experimental model and subject details

Animals

Wild-type strains were *C. elegans* variety Bristol strain N2. Worms were maintained according to standard methods. Worms were grown at 20°C on nematode growth media (NGM) plates seeded with *E. coli* (OP50) as a food source except where HB101 *E. coli* was utilized for the electrophysiology study.

Constructing a conditional knockout using the Cre-loxP system

unc-43 *conditional knockout*

According to wormbase, *unc-43* has 36 splice isoforms. Many short isoforms do not contain the kinase domain that was shown to be required for UNC-43/CaMKII's physiological functions (Rosenberg et al., 2005). Among the long isoforms, the UNC-43(K11E8.1d) and UNC-43(K11E8.1g) had been shown to mediate UNC-43/CaMKII's regulatory roles at NMJs. UNC-43(K11E8.1d) and UNC-43(K11E8.1g) are able to rescue the defects of the cholinergic transmission (Liu et al., 2007) and GABAergic synaptogenesis in the *unc-43* loss-of-function mutants (Caylor et al., 2013). To conditionally knock out *unc-43* (encoding K11E8.1d and K11E8.1g), we inserted the first loxP about 3,300 bp upstream of *unc-43* (K11E8.1b to K11E8.1l) coding sequence and the second loxP was inserted into the first intron. With the recombinase Cre expression, a 59-bp coding sequence including the start codon of UNC-43 (K11E8.1d and K11E8.1g) is deleted (Hao et al., 2023).

TRA-2 *conditional knockout*

To delete the C-terminus of TRA-2A that is critical for sex determination (Mehra et al., 1999; Okkema and Kimble, 1991), we inserted the first loxP into the 20th intron and the second loxP downstream of the 3′ UTR (C15F1.3a). With the action of Cre recombinase (Kage-Nakadai et al., 2014), the C-terminus of *TRA-2A* (Val1094 to Val1475) and whole *TRA-2C* are deleted.

Split GFP complementary system

The *xj1455[GFP11*7-unc-43]* and *xj1544[unc-57::GFP11x7]* alleles were generated for labeling endogenous UNC-43 and UNC-57 at cholinergic and GABAergic synapses. For *xj1455[GFP11*7-unc-43]*, seven copies of the GFP11 coding sequence were inserted at the N-terminus of the *unc-43* genomic locus. Briefly, GGGS (linker)-GFP11*7-GGGS (linker) coding sequence was inserted after the start codon of *unc-43* isoforms (K11E8.1b to K11E8.1l; Hao et al., 2023).

For *xj1544[unc-57::GFP11x7]*, seven copies of the GFP11 coding sequence were inserted at the C-terminus of the *unc-57* genomic locus. Briefly, GGGS (linker)-GFP11*7 coding sequence was inserted before the stop codon of *unc-57* isoforms (T04D1.3a to T04D1.3d; Hao et al., 2023).

In parallel, the GFP1-10 fragment was constitutively expressed in the GABAergic motor neurons under *unc-25* promoter or cholinergic neurons under *unc-129* promoter.

Aldicarb assay

Aldicarb (ApexBio) was dissolved in ethyl alcohol and added to NGM at a final concentration of 1.4 mM. These plates (35 mm) were seeded with 75 µl OP50 and allowed to dry overnight before use. More than 25 animals at the young-adult stage were placed on an aldicarb plate for aldicarb assay. Animals were scored as paralyzed when their head and tail did not swing for a 3 s duration. For uncoordinated mutant animals (such as *unc-29* and *acr-16* mutants), we followed the protocol from the previous report that animals were scored as paralyzed when they did not move when prodded with a platinum wire (Huang et al., 2019). The number of paralyzed animals was assessed every 10 min. At least three double-blind replicates were tested for each group.

Fluorescent microscopy imaging

Worms were anesthetized using 30 g/liter 2,3-butanedione monoxime (Sigma-Aldrich) and mounted on 2% agar on glass slides. Image acquisition was performed at 20°C on either an Olympus microscope (BX53) equipped with a 100× (NA = 1.4) oil objective, X-Cite 120LED boost high-power LED illumination system (Excelitas), and a complementary metal-oxide-semiconductor camera (Prime 95B; Photometrics), or on a Nikon spinning-disk confocal system (CSU-W1; Yokogawa) equipped with a Nikon 60× (NA = 1.4) oil objective, iChrome MLE laser (Toptica) of 488- and 561-nm excitation wavelengths, and a complementary metal-oxide-semiconductor camera (Photometrics, Prime 95B). Acquisition control was performed using Olympus cellSens Dimension 1.18 or Nikon NIS-Elements. The mean fluorescence intensities of reference FluoSphere microspheres (Thermo Fisher Scientific) were measured during each experiment and controlled for changes in illumination intensities.

Multidimensional data were reconstructed as maximum intensity projections using Metamorph software (Molecular Devices). Puncta were quantified by scanning the original full Z-stack for distinct dots in the dorsal cord. The background was subtracted with the Subtract Background tool of Image J (rolling ball radius 50 pixels) as previously reported (Pinan-Lucarré et al., 2014). Line scans were analyzed in Igor Pro (WaveMetrics) using a custom script (Dittman and Kaplan, 2006). Briefly, two image parameters were defined: "Puncta fluorescence intensity," defined as absolute peak fluorescence that is normalized to the FluoSphere microspheres standard, and "density," which is the number of peaks found per 10 µm of cord analyzed.

Adult locomotion analysis

Young-adult worms were allowed 1 min to recover from the mechanical stimulus of being moved to the assay plate before recording. All assays were performed at 20°C on NGM plates without *E. coli*. Animal locomotion was recorded at a rate of 10 frames per second (fps) for 1 min by the detecting system comprised of a FireWire camera (BioHD-EPS; Fluoca), microscope (MVX10; Olympus), and motorized stage (00-24-578-0000; Marzhauser). Acquisition control was performed using VisiView. The mean body-bend curvature and crawling locomotion velocity were analyzed by WormLab software developed by MBF Bioscience.

Scanning electron microscopy (SEM)

Young-adult hermaphrodites and males were subjected to high-pressure freezing (HPF) fixation (Cook et al., 2019; Mulcahy et al., 2018; Yu et al., 2018). Briefly, 20 animals were loaded into the 100 µm specimen chambers filled with *E. coli* and frozen under high pressure (Leica EM ICE; Leica). Then, the specimens were transferred under liquid nitrogen and freeze-substitution (EM AFS2; Leica) was performed with 2% osmium and 1% uranyl acetate for 4–5 d. Fixed animals were then washed with pyruvic acid and embedded in resin at 60°C for 48 h. Ultrathin serial sections (50 nm) were cut and glued to a wafer and counterstained in 0.08 mol/liter citrate for 10 min. Images were obtained on a GeminiSEM460 scanning electron microscope operating at 5 kV, and 3D reconstruction was performed by AMIRA software. Cholinergic synapses were identified by morphology and anatomical position, and an NMJ synapse containing a dense projection was identified from a set of serial sections, each containing a 50 nm synaptic profile. We selected the 50 nm profiles with the most apparent presynaptic specialization (dense projection) to count the synaptic vesicles (SVs), docked synaptic vesicles (DSVs), dense core vesicles (DCVs), and synaptic profile areas as previously reported (Gracheva et al., 2006; Steuer Costa et al., 2017; Xuan et al., 2017).

The synaptic vesicles (SVs) are identified as spherical, light tray structures with an average diameter of around 30 nm; the docked synaptic vesicles (DSVs) are defined as 0 nm separation between vesicle and plasma membrane as in the previous report (Gracheva et al., 2010; Stigloher et al., 2011; Xuan et al., 2017); the dense core vesicles (DCVs) were identified as spherical, dark black structures with thick membranes and an average diameter of ~60–70 nm. The number of SVs, DSVs, and DCVs are normalized to the area of the synaptic profile as reported (Gracheva et al., 2006; Steuer Costa et al., 2017; Xuan et al., 2017). The numbers of synapses analyzed for each genotype were marked in the figure, and three to four animals were used for each condition.

Electrophysiology

Worms were superfused in the extracellular solution (127 mM NaCl, 5 mM KCl, 26 mM $NaHCO_3$, 1.25 mM NaH_2PO_4, 20 mM glucose, 1 mM $CaCl_2$, and 4 mM $MgCl_2$, bubbled with 5% CO_2 and 95% O_2 at 22°C), and the internal solution contained 105 mM CH_3O_3SCs, 10 mM CsCl, 15 mM CsF, 4 mM $MgCl_2$, 5 mM EGTA, 0.25 mM $CaCl_2$, 10 mM HEPES, and 4 mM Na_2ATP. The solution was adjusted to pH 7.2 using CsOH. Whole-cell recordings were carried out at −60 mV for mEPSCs and 0 mV for mIPSCs.

RNAi feeding

The *unc-43* RNAi feeding was performed following the previously established protocol (Kamath et al., 2003). The *unc-43* RNAi and control (empty vector) bacteria were seeded on RNAi-feeding NGM plates supplemented with 1 mM IPTG and incubated overnight at 20°C to induce dsRNA expression. Adult animals were then transferred to the RNAi plates for 2 h to remove residual OP50 bacteria. Subsequently, they were transferred to a new RNAi plate and allowed to lay eggs for 2 h. Their progenies were used for the subsequent experiment.

Statistics

All data are reported as mean ± SEM (standard error of the mean). Statistical analyses were performed using GraphPad Prism (version 8). Data distribution was assumed to be normal but this was not formally tested. We calculated P values by two-way ANOVA (Figs. 1 F, 2, A and B, and 8 B; and Figs. S1, B–G, S4, B–H, and S5, F and G), one-way ANOVA with Bonferroni's multiple comparisons test (Figs. 2, D and E, 5, C and D, 6, B, C, and E–I, 7, C–G, and 8, C, E, and F; and Figs. S3, D, E, and G–I, S4 J, and S5 E), one-way ANOVA with Dunnett's multiple comparisons test (Fig. 7, C and D), or two-tailed and unpaired Student's *t* test (Fig. 1, C–E, H, I, K, and L, 3, C, D, F, and G, 4, B and D, and 5, F and G; and Fig. S2, B and C). In all figures, P values are denoted as * < 0.05, ** < 0.01, *** < 0.001.

Online supplemental material

Fig. S1 shows that sexually dimorphic synaptic transmission at NMJs arises at the L4 stage and exists in various other natural strains. Fig. S2 shows the ultrastructural analysis of synapses at NMJs. Fig. S3 shows UNC-43/CaMKII mediates the sexually dimorphic cholinergic transmission. Fig. S4 shows that sex-specific factors and CA neurons do not mediate the sexually dimorphic cholinergic transmission at NMJs. Fig. S5 shows conditional knockout of *tra-2* leads to a neuron-specific degradation of TRA-1. Table S1 shows the reagents or resources used in this study. Table S2 shows the strains used in this study. Table S3 shows the plasmids and primers used in this study. Table S4 shows the software and algorithms used in this study.

Data availability

The data generated are available in the published article, its online supplemental material, or available from the authors upon reasonable request.

Acknowledgments

We thank the *C. elegans* Genetics Stock Center, National Bio-Resource Project (NBRP), Dr. Douglas Stuart Portman, Dr. Jean-Louis Bessereau, Dr. Joshua Kaplan, Dr. Yan Zou, Dr. Billy Yingchuan Qi, and Dr. Quan Wen for sharing strains and reagents. We also thank the Molecular Imaging Core Facility (MICF), the Molecular and Cell Biology Core Facility (MCB), and the Bio-Electron Microscopy Facility at the School of Life Science and Technology, ShanghaiTech University for help in imaging and FACS sorting. We would like to thank Dr. Yu Kong and Lijun Pan (Electron Microscopy Facilities of Center for Excellence in Brain Science and Technology, Chinese Academy of Science) for assistance with SEM sample preparation and image analysis.

This work was supported by the National Key Research and Development Program of China (2021ZD0202500), the National Natural Science Foundation of China (32170963 to X.-J. Tong), the Science and Technology Commission of Shanghai Municipality (21ZR1481000 to X.-J. Tong), and the National Health and Medical Research Council (GNT1122351 to Z. Hu).

Author contributions: W.-X. Zeng, H. Liu, Y. Hao, K.-Y. Qian, F.-M. Tian, L. Li, B. Yu, and X.-T. Zeng designed, performed, and analyzed the experiments. W.-X. Zeng, Y. Hao, K.-Y. Qian, F.-M. Tian, and X.-T. Zeng performed the aldicarb experiments, fluorescent imaging, calcium imaging, locomotion analysis, and SEM analysis. H. Liu, L. Li, and B. Yu performed electrophysiological recordings. S. Gao, Z. Hu, and X.-J. Tong supervised the experimental design and data interpretation. W.-X. Zeng, Y. Hao, K.-Y. Qian, and X.-J. Tong wrote the manuscript. All authors discussed the results and commented on the manuscript.

Disclosures: The authors declare no competing interests exist.

Submitted: 27 January 2023
Revised: 20 June 2023
Accepted: 14 August 2023

References

Asahina, K., K. Watanabe, B.J. Duistermars, E. Hoopfer, C.R. González, E.A. Eyjólfsdóttir, P. Perona, and D.J. Anderson. 2014. Tachykinin-expressing neurons control male-specific aggressive arousal in *Drosophila*. *Cell*. 156: 221–235. https://doi.org/10.1016/j.cell.2013.11.045

Bourgeron, T. 2015. From the genetic architecture to synaptic plasticity in autism spectrum disorder. *Nat. Rev. Neurosci.* 16:551–563. https://doi.org/10.1038/nrn3992

Cabantous, S., T.C. Terwilliger, and G.S. Waldo. 2005. Protein tagging and detection with engineered self-assembling fragments of green fluorescent protein. *Nat. Biotechnol.* 23:102–107. https://doi.org/10.1038/nbt1044

Cachero, S., A.D. Ostrovsky, J.Y. Yu, B.J. Dickson, and G.S.X.E. Jefferis. 2010. Sexual dimorphism in the fly brain. *Curr. Biol.* 20:1589–1601. https://doi.org/10.1016/j.cub.2010.07.045

Carrillo, R.A., D.P. Olsen, K.S. Yoon, and H. Keshishian. 2010. Presynaptic activity and CaMKII modulate retrograde semaphorin signaling and synaptic refinement. *Neuron*. 68:32–44. https://doi.org/10.1016/j.neuron.2010.09.005

Caylor, R.C., Y. Jin, and B.D. Ackley. 2013. The *Caenorhabditis elegans* voltage-gated calcium channel subunits UNC-2 and UNC-36 and the calcium-dependent kinase UNC-43/CaMKII regulate neuromuscular junction morphology. *Neural Dev.* 8:10. https://doi.org/10.1186/1749-8104-8-10

Chen, P.B., R.K. Hu, Y.E. Wu, L. Pan, S. Huang, P.E. Micevych, and W. Hong. 2019. Sexually dimorphic control of parenting behavior by the medial amygdala. *Cell*. 176:1206–1221.e18. https://doi.org/10.1016/j.cell.2019.01.024

Cline, T.W., and B.J. Meyer. 1996. Vive la différence: Males vs females in flies vs worms. *Annu. Rev. Genet.* 30:637–702. https://doi.org/10.1146/annurev.genet.30.1.637

Cook, S.J., T.A. Jarrell, C.A. Brittin, Y. Wang, A.E. Bloniarz, M.A. Yakovlev, K.C.Q. Nguyen, L.T.H. Tang, E.A. Bayer, J.S. Duerr, et al. 2019. Whole-animal connectomes of both *Caenorhabditis elegans* sexes. *Nature*. 571: 63–71. https://doi.org/10.1038/s41586-019-1352-7

Dittman, J.S., and J.M. Kaplan. 2006. Factors regulating the abundance and localization of synaptobrevin in the plasma membrane. *Proc. Natl. Acad. Sci. USA*. 103:11399–11404. https://doi.org/10.1073/pnas.0600784103

Emmons, S.W. 2014. The development of sexual dimorphism: Studies of the *Caenorhabditis elegans* male. *Wiley Interdiscip. Rev. Dev. Biol.* 3:239–262. https://doi.org/10.1002/wdev.136

Emmons, S.W. 2018. Neural circuits of sexual behavior in *Caenorhabditis elegans*. *Annu. Rev. Neurosci.* 41:349–369. https://doi.org/10.1146/annurev-neuro-070815-014056

Fagan, K.A., and D.S. Portman. 2014. Sexual modulation of neural circuits and behavior in *Caenorhabditis elegans*. *Semin. Cell Dev. Biol.* 33:3–9. https://doi.org/10.1016/j.semcdb.2014.06.007

García, L.R., and D.S. Portman. 2016. Neural circuits for sexually dimorphic and sexually divergent behaviors in *Caenorhabditis elegans*. *Curr. Opin. Neurobiol.* 38:46–52. https://doi.org/10.1016/j.conb.2016.02.002

Ge, J.F., C.C. Qi, J.P. Qiao, C.W. Wang, and N.J. Zhou. 2013. Sex differences in ICR mice in the Morris water maze task. *Physiol. Res.* 62:107–117. https://doi.org/10.33549/physiolres.932371

Gracheva, E.O., A.O. Burdina, A.M. Holgado, M. Berthelot-Grosjean, B.D. Ackley, G. Hadwiger, M.L. Nonet, R.M. Weimer, and J.E. Richmond. 2006. Tomosyn inhibits synaptic vesicle priming in *Caenorhabditis elegans*. *PLoS Biol.* 4:e261. https://doi.org/10.1371/journal.pbio.0040261

Gracheva, E.O., E.B. Maryon, M. Berthelot-Grosjean, and J.E. Richmond. 2010. Differential regulation of synaptic vesicle tethering and docking by UNC-18 and TOM-1. *Front. Synaptic Neurosci.* 2:141. https://doi.org/10.3389/fnsyn.2010.00141

Hao, Y., H. Liu, X.-T. Zeng, Y. Wang, W.-X. Zeng, K.-Y. Qian, L. Li, M.-X. Chi, S. Gao, Z. Hu, and X.-J. Tong. 2023. UNC-43/CaMKII-triggered anterograde signals recruit GABAARs to mediate inhibitory synaptic transmission and plasticity at *C. elegans* NMJs. *Nat. Commun.* 14:1436. https://doi.org/10.1038/s41467-023-37137-0

Hart, M.P., and O. Hobert. 2015. Sexual dimorphism: Mystery neurons control sex-specific behavioral plasticity. *Curr. Biol.* 25:R1170–R1172. https://doi.org/10.1016/j.cub.2015.11.002

Hiller, R.M., R.L. Young, and N. Weber. 2016. Sex differences in pre-diagnosis concerns for children later diagnosed with autism spectrum disorder. *Autism*. 20:75–84. https://doi.org/10.1177/1362361314568899

Hodgkin, J. 1987. A genetic analysis of the sex-determining gene, tra-1, in the nematode *Caenorhabditis elegans*. *Genes Dev.* 1:731–745. https://doi.org/10.1101/gad.1.7.731

Hojjati, M.R., G.M. van Woerden, W.J. Tyler, K.P. Giese, A.J. Silva, L. Pozzo-Miller, and Y. Elgersma. 2007. Kinase activity is not required for alphaCaMKII-dependent presynaptic plasticity at CA3-CA1 synapses. *Nat. Neurosci.* 10:1125–1127. https://doi.org/10.1038/nn1946

Hoover, C.M., S.L. Edwards, S.C. Yu, M. Kittelmann, J.E. Richmond, S. Eimer, R.M. Yorks, and K.G. Miller. 2014. A novel CaM kinase II pathway controls the location of neuropeptide release from *Caenorhabditis elegans* motor neurons. *Genetics*. 196:745–765. https://doi.org/10.1534/genetics.113.158568

Houser, C.R., G.D. Crawford, P.M. Salvaterra, and J.E. Vaughn. 1985. Immunocytochemical localization of choline acetyltransferase in rat cerebral cortex: A study of cholinergic neurons and synapses. *J. Comp. Neurol.* 234:17–34. https://doi.org/10.1002/cne.902340103

Howard, D.M., M.J. Adams, M. Shirali, T.K. Clarke, R.E. Marioni, G. Davies, J.R.I. Coleman, C. Alloza, X. Shen, M.C. Barbu, et al. 2018. Genome-wide association study of depression phenotypes in UK Biobank identifies variants in excitatory synaptic pathways. *Nat. Commun.* 9:1470. https://doi.org/10.1038/s41467-018-03819-3

Huang, Y.C., J.K. Pirri, D. Rayes, S. Gao, B. Mulcahy, J. Grant, Y. Saheki, M.M. Francis, M. Zhen, and M.J. Alkema. 2019. Gain-of-function mutations in the UNC-2/CaV2α channel lead to excitation-dominant synaptic transmission in *Caenorhabditis elegans*. *Elife*. 8:e45905. https://doi.org/10.7554/eLife.45905

Hunter, C.P., and W.B. Wood. 1990. The tra-1 gene determines sexual phenotype cell-autonomously in *C. elegans*. *Cell*. 63:1193–1204. https://doi.org/10.1016/0092-8674(90)90415-B

Iossifov, I., M. Ronemus, D. Levy, Z. Wang, I. Hakker, J. Rosenbaum, B. Yamrom, Y.H. Lee, G. Narzisi, A. Leotta, et al. 2012. De novo gene disruptions in children on the autistic spectrum. *Neuron*. 74:285–299. https://doi.org/10.1016/j.neuron.2012.04.009

Kage-Nakadai, E., R. Imae, Y. Suehiro, S. Yoshina, S. Hori, and S. Mitani. 2014. A conditional knockout toolkit for *Caenorhabditis elegans* based on the Cre/loxP recombination. *PLoS One*. 9:e114680. https://doi.org/10.1371/journal.pone.0114680

Kalis, A.K., D.U. Kissiov, E.S. Kolenbrander, Z. Palchick, S. Raghavan, B.J. Tetreault, E. Williams, C.M. Loer, and J.R. Wolff. 2014. Patterning of sexually dimorphic neurogenesis in the *Caenorhabditis elegans* ventral cord by Hox and TALE homeodomain transcription factors. *Dev. Dyn.* 243:159–171. https://doi.org/10.1002/dvdy.24064

Kamath, R.S., A.G. Fraser, Y. Dong, G. Poulin, R. Durbin, M. Gotta, A. Kanapin, N. Le Bot, S. Moreno, M. Sohrmann, et al. 2003. Systematic functional analysis of the *Caenorhabditis elegans* genome using RNAi. *Nature*. 421:231–237. https://doi.org/10.1038/nature01278

Kamiyama, D., S. Sekine, B. Barsi-Rhyne, J. Hu, B. Chen, L.A. Gilbert, H. Ishikawa, M.D. Leonetti, W.F. Marshall, J.S. Weissman, and B. Huang. 2016. Versatile protein tagging in cells with split fluorescent protein. *Nat. Commun.* 7:11046. https://doi.org/10.1038/ncomms11046

Kang, H.J., B. Voleti, T. Hajszan, G. Rajkowska, C.A. Stockmeier, P. Licznerski, A. Lepack, M.S. Majik, L.S. Jeong, M. Banasr, et al. 2012. Decreased expression of synapse-related genes and loss of synapses in major depressive disorder. *Nat. Med.* 18:1413–1417. https://doi.org/10.1038/nm.2886

Kelley, D.B. 1988. Sexually dimorphic behaviors. *Annu. Rev. Neurosci.* 11:225–251. https://doi.org/10.1146/annurev.ne.11.030188.001301

Kessler, R.C., K.A. McGonagle, M. Swartz, D.G. Blazer, and C.B. Nelson. 1993. Sex and depression in the national comorbidity survey. I: Lifetime prevalence, chronicity and recurrence. *J. Affect. Disord.* 29:85–96. https://doi.org/10.1016/0165-0327(93)90026-G

Kim, B., B. Suo, and S.W. Emmons. 2016. Gene function prediction based on developmental transcriptomes of the two sexes in *C. elegans*. *Cell Rep.* 17:917–928. https://doi.org/10.1016/j.celrep.2016.09.051

Lawson, H., E. Vuong, R.M. Miller, K. Kiontke, D.H. Fitch, and D.S. Portman. 2019. The Makorin lep-2 and the lncRNA lep-5 regulate lin-28 to schedule sexual maturation of the *C. elegans* nervous system. *Elife*. 8:e43660. https://doi.org/10.7554/eLife.43660

Lima Caldeira, G., J. Peça, and A.L. Carvalho. 2019. New insights on synaptic dysfunction in neuropsychiatric disorders. *Curr. Opin. Neurobiol.* 57:62–70. https://doi.org/10.1016/j.conb.2019.01.004

Lisman, J., H. Schulman, and H. Cline. 2002. The molecular basis of CaMKII function in synaptic and behavioural memory. *Nat. Rev. Neurosci.* 3:175–190. https://doi.org/10.1038/nrn753

Lisman, J., R. Yasuda, and S. Raghavachari. 2012. Mechanisms of CaMKII action in long-term potentiation. *Nat. Rev. Neurosci.* 13:169–182. https://doi.org/10.1038/nrn3192

Liu, Q., B. Chen, Q. Ge, and Z.W. Wang. 2007. Presynaptic Ca^{2+}/calmodulin-dependent protein kinase II modulates neurotransmitter release by activating BK channels at *Caenorhabditis elegans* neuromuscular junction. *J. Neurosci.* 27:10404–10413. https://doi.org/10.1523/JNEUROSCI.5634-06.2007

Mahoney, T.R., S. Luo, and M.L. Nonet. 2006. Analysis of synaptic transmission in *Caenorhabditis elegans* using an aldicarb-sensitivity assay. *Nat. Protoc.* 1:1772–1777. https://doi.org/10.1038/nprot.2006.281

Markert, S.M., M. Skoruppa, B. Yu, B. Mulcahy, M. Zhen, S. Gao, M. Sendtner, and C. Stigloher. 2020. Overexpression of an ALS-associated FUS mutation in *C. elegans* disrupts NMJ morphology and leads to defective neuromuscular transmission. *Biol. Open*. 9:bio055129. https://doi.org/10.1242/bio.055129

McFadyen, M.P., G. Kusek, V.J. Bolivar, and L. Flaherty. 2003. Differences among eight inbred strains of mice in motor ability and motor learning on a rotorod. *Genes Brain Behav.* 2:214–219. https://doi.org/10.1034/j.1601-183X.2003.00028.x

Mehra, A., J. Gaudet, L. Heck, P.E. Kuwabara, and A.M. Spence. 1999. Negative regulation of male development in *Caenorhabditis elegans* by a protein-protein interaction between TRA-2A and FEM-3. *Genes Dev.* 13:1453–1463. https://doi.org/10.1101/gad.13.11.1453

Moro, A., G.M. van Woerden, R.F. Toonen, and M. Verhage. 2020. CaMKII controls neuromodulation via neuropeptide gene expression and axonal targeting of neuropeptide vesicles. *PLoS Biol.* 18:e3000826. https://doi.org/10.1371/journal.pbio.3000826

Mowrey, W.R., J.R. Bennett, and D.S. Portman. 2014. Distributed effects of biological sex define sex-typical motor behavior in *Caenorhabditis elegans*. *J. Neurosci.* 34:1579–1591. https://doi.org/10.1523/JNEUROSCI.4352-13.2014

Mulcahy, B., D. Witvliet, D. Holmyard, J. Mitchell, A.D. Chisholm, Y. Meirovitch, A.D.T. Samuel, and M. Zhen. 2018. A pipeline for volume electron microscopy of the *Caenorhabditis elegans* nervous system. *Front. Neural Circuits*. 12:94. https://doi.org/10.3389/fncir.2018.00094

O'Leary, T.P., H.M. Mantolino, K.R. Stover, and R.E. Brown. 2020. Age-related deterioration of motor function in male and female 5xFAD mice from 3 to 16 months of age. *Genes Brain Behav.* 19:e12538. https://doi.org/10.1111/gbb.12538

Ohgi, Y., T. Futamura, and K. Hashimoto. 2015. Glutamate signaling in synaptogenesis and NMDA receptors as potential therapeutic targets for psychiatric disorders. *Curr. Mol. Med.* 15:206–221. https://doi.org/10.2174/1566524015666150330143008

Okkema, P.G., and J. Kimble. 1991. Molecular analysis of tra-2, a sex determining gene in *C. elegans*. *EMBO J.* 10:171–176. https://doi.org/10.1002/j.1460-2075.1991.tb07933.x

Oren-Suissa, M., E.A. Bayer, and O. Hobert. 2016. Sex-specific pruning of neuronal synapses in *Caenorhabditis elegans*. *Nature*. 533:206–211. https://doi.org/10.1038/nature17977

Peedikayil-Kurien, S., H. Setty, and M. Oren-Suissa. 2022. Environmental experiences shape sexually dimorphic neuronal circuits and behaviour. *FEBS J.* https://doi.org/10.1111/febs.16714

Pereira, L., F. Aeschimann, C. Wang, H. Lawson, E. Serrano-Saiz, D.S. Portman, H. Großhans, and O. Hobert. 2019. Timing mechanism of sexually dimorphic nervous system differentiation. *Elife*. 8:e42078. https://doi.org/10.7554/eLife.42078

Pinan-Lucarré, B., H. Tu, M. Pierron, P.I. Cruceyra, H. Zhan, C. Stigloher, J.E. Richmond, and J.L. Bessereau. 2014. *C. elegans* Punctin specifies cholinergic versus GABAergic identity of postsynaptic domains. *Nature*. 511:466–470. https://doi.org/10.1038/nature13313

Qian, K.Y., W.X. Zeng, Y. Hao, X.T. Zeng, H. Liu, L. Li, L. Chen, F.M. Tian, C. Chang, Q. Hall, et al. 2021. Male pheromones modulate synaptic transmission at the *C. elegans* neuromuscular junction in a sexually dimorphic manner. *Elife*. 10:e67170. https://doi.org/10.7554/eLife.67170

Richmond, J.E., and E.M. Jorgensen. 1999. One GABA and two acetylcholine receptors function at the *C. elegans* neuromuscular junction. *Nat. Neurosci.* 2:791–797. https://doi.org/10.1038/12160

Ringstad, N., H. Gad, P. Löw, G. Di Paolo, L. Brodin, O. Shupliakov, and P. De Camilli. 1999. Endophilin/SH3p4 is required for the transition from early to late stages in clathrin-mediated synaptic vesicle endocytosis. *Neuron*. 24:143–154. https://doi.org/10.1016/S0896-6273(00)80828-4

Rosenberg, O.S., S. Deindl, R.J. Sung, A.C. Nairn, and J. Kuriyan. 2005. Structure of the autoinhibited kinase domain of CaMKII and SAXS analysis of the holoenzyme. *Cell*. 123:849–860. https://doi.org/10.1016/j.cell.2005.10.029

Ryan, D.A., R.M. Miller, K. Lee, S.J. Neal, K.A. Fagan, P. Sengupta, and D.S. Portman. 2014. Sex, age, and hunger regulate behavioral prioritization through dynamic modulation of chemoreceptor expression. *Curr. Biol.* 24:2509–2517. https://doi.org/10.1016/j.cub.2014.09.032

Salzberg, Y., V. Pechuk, A. Gat, H. Setty, S. Sela, and M. Oren-Suissa. 2020. Synaptic protein degradation controls sexually dimorphic circuits through regulation of DCC/UNC-40. *Curr. Biol.* 30:4128–4141.e5. https://doi.org/10.1016/j.cub.2020.08.002

Schmidt, A., M. Wolde, C. Thiele, W. Fest, H. Kratzin, A.V. Podtelejnikov, W. Witke, W.B. Huttner, and H.D. Söling. 1999. Endophilin I mediates synaptic vesicle formation by transfer of arachidonate to lysophosphatidic acid. *Nature*. 401:133–141. https://doi.org/10.1038/43613

Schuske, K.R., J.E. Richmond, D.S. Matthies, W.S. Davis, S. Runz, D.A. Rube, A.M. van der Bliek, and E.M. Jorgensen. 2003. Endophilin is required for synaptic vesicle endocytosis by localizing synaptojanin. *Neuron*. 40:749–762. https://doi.org/10.1016/S0896-6273(03)00667-6

Schvarzstein, M., and A.M. Spence. 2006. The *C. elegans* sex-determining GLI protein TRA-1A is regulated by sex-specific proteolysis. *Dev. Cell*. 11:733–740. https://doi.org/10.1016/j.devcel.2006.09.017

Serrano-Saiz, E., M. Oren-Suissa, E.A. Bayer, and O. Hobert. 2017. Sexually dimorphic differentiation of a *C. elegans* hub neuron is cell autonomously

controlled by a conserved transcription factor. *Curr. Biol.* 27:199–209. https://doi.org/10.1016/j.cub.2016.11.045

Sheng, M., and C.C. Hoogenraad. 2007. The postsynaptic architecture of excitatory synapses: A more quantitative view. *Annu. Rev. Biochem.* 76: 823–847. https://doi.org/10.1146/annurev.biochem.76.060805.160029

Siksou, L., P. Rostaing, J.P. Lechaire, T. Boudier, T. Ohtsuka, A. Fejtová, H.T. Kao, P. Greengard, E.D. Gundelfinger, A. Triller, and S. Marty. 2007. Three-dimensional architecture of presynaptic terminal cytomatrix. *J. Neurosci.* 27:6868–6877. https://doi.org/10.1523/JNEUROSCI.1773-07.2007

Simerly, R.B. 2002. Wired for reproduction: Organization and development of sexually dimorphic circuits in the mammalian forebrain. *Annu. Rev. Neurosci.* 25:507–536. https://doi.org/10.1146/annurev.neuro.25.112701.142745

Starostina, N.G., J.M. Lim, M. Schvarzstein, L. Wells, A.M. Spence, and E.T. Kipreos. 2007. A CUL-2 ubiquitin ligase containing three FEM proteins degrades TRA-1 to regulate *C. elegans* sex determination. *Dev. Cell.* 13: 127–139. https://doi.org/10.1016/j.devcel.2007.05.008

Steuer Costa, W., S.C. Yu, J.F. Liewald, and A. Gottschalk. 2017. Fast cAMP modulation of neurotransmission via neuropeptide signals and vesicle loading. *Curr. Biol.* 27:495–507. https://doi.org/10.1016/j.cub.2016.12.055

Stigloher, C., H. Zhan, M. Zhen, J. Richmond, and J.L. Bessereau. 2011. The presynaptic dense projection of the *Caenorhabditis elegans* cholinergic neuromuscular junction localizes synaptic vesicles at the active zone through SYD-2/liprin and UNC-10/RIM-dependent interactions. *J. Neurosci.* 31:4388–4396. https://doi.org/10.1523/JNEUROSCI.6164-10.2011

Takemoto-Kimura, S., K. Suzuki, S.I. Horigane, S. Kamijo, M. Inoue, M. Sakamoto, H. Fujii, and H. Bito. 2017. Calmodulin kinases: Essential regulators in health and disease. *J. Neurochem.* 141:808–818. https://doi.org/10.1111/jnc.14020

Taylor, S.R., G. Santpere, A. Weinreb, A. Barrett, M.B. Reilly, C. Xu, E. Varol, P. Oikonomou, L. Glenwinkel, R. McWhirter, et al. 2021. Molecular topography of an entire nervous system. *Cell.* 184:4329–4347.e23. https://doi.org/10.1016/j.cell.2021.06.023

Tejos-Bravo, M., R.H. Oakley, S.D. Whirledge, W.A. Corrales, J.P. Silva, G. García-Rojo, J. Toledo, W. Sanchez, L. Román-Albasini, E. Aliaga, et al. 2021. Deletion of hippocampal Glucocorticoid receptors unveils sex-biased microRNA expression and neuronal morphology alterations in mice. *Neurobiol. Stress.* 14:100306. https://doi.org/10.1016/j.ynstr.2021.100306

Van Wijngaarden-Cremers, P.J.M., E. van Eeten, W.B. Groen, P.A. Van Deurzen, I.J. Oosterling, and R.J. Van der Gaag. 2014. Gender and age differences in the core triad of impairments in autism spectrum disorders: A systematic review and meta-analysis. *J. Autism Dev. Disord.* 44: 627–635. https://doi.org/10.1007/s10803-013-1913-9

Wan, X., Y. Zhou, C.M. Chan, H. Yang, C. Yeung, and K.L. Chow. 2019. SRD-1 in AWA neurons is the receptor for female volatile sex pheromones in *C. elegans* males. *EMBO Rep.* 20:e46288. https://doi.org/10.15252/embr.201846288

Wang, C., and O. Hobert. 2019. Sex-specific pheromone responses in *Caenorhabditis elegans*. *EMBO Rep.* 20:e47599. https://doi.org/10.15252/embr.201847599

White, J.G., E. Southgate, J.N. Thomson, and S. Brenner. 1986. The structure of the nervous system of the nematode *Caenorhabditis elegans*. *Philos. Trans. R. Soc. Lond. B Biol. Sci.* 314:1–340. https://doi.org/10.1098/rstb.1986.0056

Xuan, Z., L. Manning, J. Nelson, J.E. Richmond, D.A. Colón-Ramos, K. Shen, and P.T. Kurshan. 2017. Clarinet (CLA-1), a novel active zone protein required for synaptic vesicle clustering and release. *Elife.* 6:e29276. https://doi.org/10.7554/eLife.29276

Yan, Z., X. Cheng, Y. Li, Z. Su, Y. Zhou, and J. Liu. 2022. Sexually dimorphic neurotransmitter release at the neuromuscular junction in adult *Caenorhabditis elegans*. *Front. Mol. Neurosci.* 14:780396. https://doi.org/10.3389/fnmol.2021.780396

Yu, S.C., B. Jánosi, J.F. Liewald, S. Wabnig, and A. Gottschalk. 2018. Endophilin A and B join forces with clathrin to mediate synaptic vesicle recycling in *Caenorhabditis elegans*. *Front. Mol. Neurosci.* 11:196. https://doi.org/10.3389/fnmol.2018.00196

Zarkower, D., and J. Hodgkin. 1992. Molecular analysis of the *C. elegans* sex-determining gene tra-1: A gene encoding two zinc finger proteins. *Cell.* 70:237–249. https://doi.org/10.1016/0092-8674(92)90099-X

Supplemental material

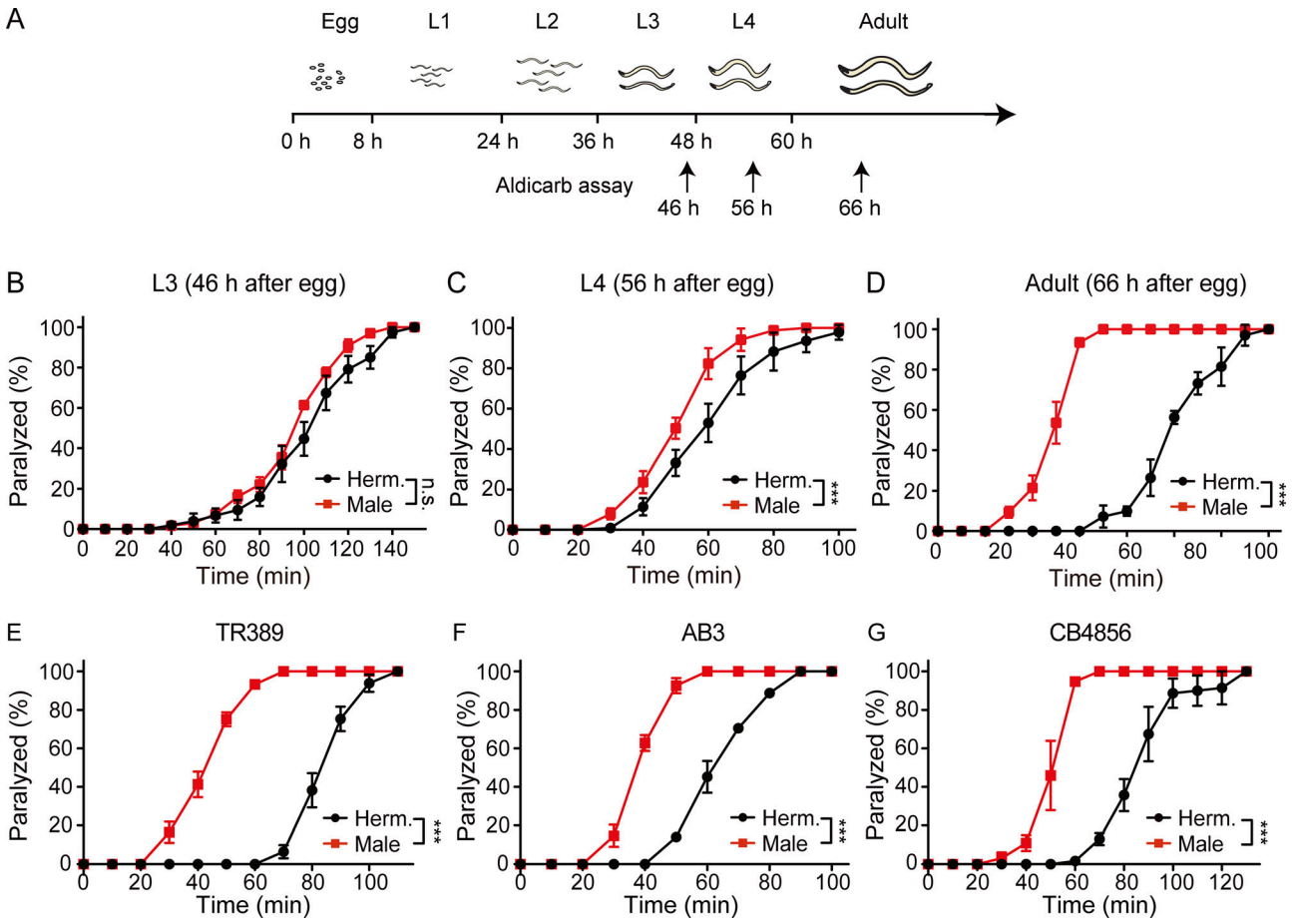

Figure S1. **The sexually dimorphic synaptic transmission at NMJs arises at the L4 stage and exists in various other natural strains. (A–D)** The sexually dimorphic synaptic transmission at NMJs arises at the L4 stage. **(A)** Schematic illustration of the life cycles of *C. elegans* and the time when the aldicarb sensitivity assay was applied. **(B–D)** Time course analysis of 1.4 mM aldicarb-induced paralysis in the L3-staged (B), L4-staged (C), and adult (D) hermaphrodites (Herm.) and males (Male). The data for the adult are the same as in Fig. 1 F. **(E–G)** The sexually dimorphic synaptic transmission at NMJs exist in various other natural strains. Time course analysis of 1.4 mM aldicarb-induced paralysis in adult hermaphrodites (Herm.) and males (Male) in TR389 (E), AB3 (F), and CB4856 (G) strains. In B–G, for each of the group, $n = 3$ biologically independent samples; each sample contains ≥25 animals. Data are presented as mean values ± SEM. Two-way ANOVA comparing all of the time points. ***P < 0.001. n.s. not significant.

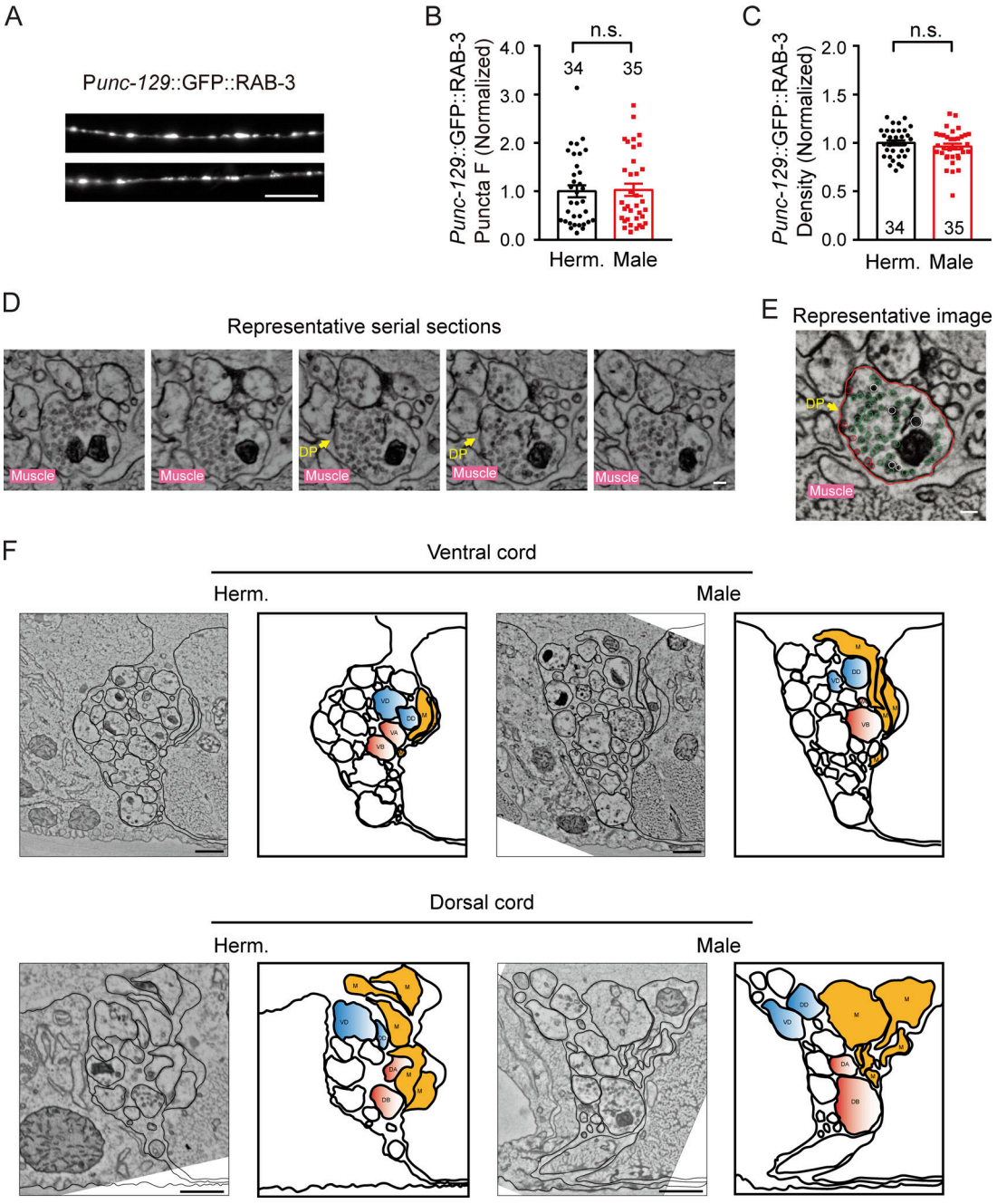

Figure S2. **Ultrastructural analysis of synapses at NMJs. (A–C)** The GFP-RAB-3 driven by *unc-129* promoter has no sex-differential expression. The puncta fluorescence intensities and densities of GFP::RAB-3 driven by *unc-129* promoter in dorsal nerve cord axons in the adult hermaphrodites (Herm.) and males (Male). Representative images (A), mean puncta intensity (B), and density (C) are shown. Scale bars, 10 µm. Data are presented as mean values ± SEM. **(D)** Representative micrographs from the serial sections with each containing a 50 nm cholinergic synaptic profile. **(E)** Representative of 50 nm cholinergic synaptic profile. Yellow arrows indicate the dense projection (DP). Scale bar, 200 nm. The representative images shown in the figure are derived from the same dataset as presented in Fig. 4, A and B. **(F)** Representative transverse section through the ventral and dorsal cord (left) and process identifications (right) in hermaphrodites (Herm.) and males. The sequence of motor neuron classes from dorsal to ventral is VD, DD, VA, and VB. NMJs are made between motor neurons and muscle arms (M). Scale bar, 500 nm. Two-tailed and unpaired Student's *t* test for B and C. n.s., not significant.

A

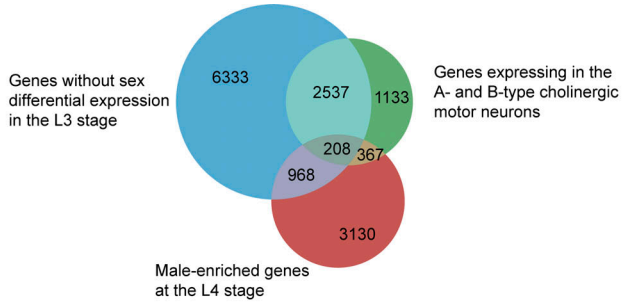

B

Genes expressed in the cholinergic motor neurons and enriched in males after the L4 stage (208)

abt-2	*dop-1*	*got-2.2*	*lin-14*	*pat-2*	*sod-3*	C05G5.1	F07H5.3	K01A11.1	T27C4.1	ZC247.1
acr-2	*dop-3*	*gpd-3*	*lin-2*	*pck-1*	*sod-4*	C07A12.2	F13H6.1	K02D10.4	T28C6.7	ZC328.2
acr-24	*dop-5*	*gsk-3*	*madd-4*	*pde-1*	*sulp-8*	C14B1.3	F14B6.2	K02F2.5	W02D9.10	ZC449.4
apl-1	*drn-1*	*gyg-1*	*mec-2*	*pdf-1*	*sup-1*	C16D9.6	F21C10.3	K07C10.3	W06H8.6	ZK1290.5
apt-9	*egl-21*	*hlh-30*	*mef-2*	*pdfr-1*	*tbc-6*	C18A11.1	F22F7.7	K11H12.7	W07G4.5	ZK54.1
arrd-6	*egl-3*	*jph-1*	*msi-1*	*pfk-1*	*tir-1*	C24A3.2	F31E3.2	K12H4.4	Y15E3A.5	ZK637.14
cab-1	*egl-8*	*kcc-2*	*nac-3*	*pgal-1*	*tos-1*	C30E1.9	F34H10.4	M176.4	Y39E4B.6	ZK673.11
cah-4	*ell-1*	*kcnl-1*	*ncam-1*	*pitp-1*	*tpa-1*	C31H5.5	F37C4.5	R02F11.3	Y39F10A.1	ZK813.4
cal-2	*fat-1*	*kin-1*	*ncx-4*	*plc-1*	*twk-18*	C33A11.1	F38B2.4	R05D7.3	Y45F10D.10	
cal-4	*flp-11*	*kin-2*	*nhr-1*	*pll-1*	*twk-29*	C34F11.3	F43C9.2	R05G6.10	Y45G5AM.3	
cha-1	*flp-9*	*klc-2*	*nhr-3*	*pme-5*	*twk-49*	C40H5.2	F46H5.3	R13H4.5	Y48C3A.3	
ckb-4	*frpr-11*	*klp-4*	*nlp-1*	*rab-37*	*unc-18*	C42C1.2	F47B8.2	T04A8.18	Y53F4B.12	
ckr-1	*frpr-16*	*ldh-1*	*nlp-13*	*rbf-1*	*unc-43*	C45G9.8	F47D12.6	T04B2.5	Y54G2A.41	
ckr-2	*gar-2*	*lec-2*	*nlp-15*	*rrc-1*	*unc-54*	C48B4.3	F49C12.12	T07C12.15	Y55F3AM.10	
clec-184	*gar-3*	*lgc-31*	*nlp-21*	*sesn-1*	*unc-58*	C54G6.3	F52A8.3	T12A7.2	Y62E10A.13	
cnb-1	*glb-15*	*lgc-33*	*nlp-38*	*sipa-1*	*ztf-22*	C54G7.1	F56A12.2	T12B3.3	Y64G10A.6	
cth-2	*glb-32*	*lgc-38*	*npr-2*	*slo-2*	B0252.8	C56G7.3	F57A8.4	T13H5.1	Y69A2AR.31	
cutl-23	*glr-4*	*lgc-41*	*npr-23*	*sma-9*	B0513.5	F02A9.1	F57B1.5	T14D7.1	Y73B6BL.35	
deb-1	*gly-5*	*lgc-47*	*npr-5*	*snt-3*	C01C4.3	F02A9.7	H10D18.5	T23B12.11	Y73E7A.3	
dlk-1	*gnrr-4*	*lim-9*	*pat-10*	*snt-5*	C02D5.4	F02E9.5	H18N23.2	T26C5.4	Y97E10AR.1	

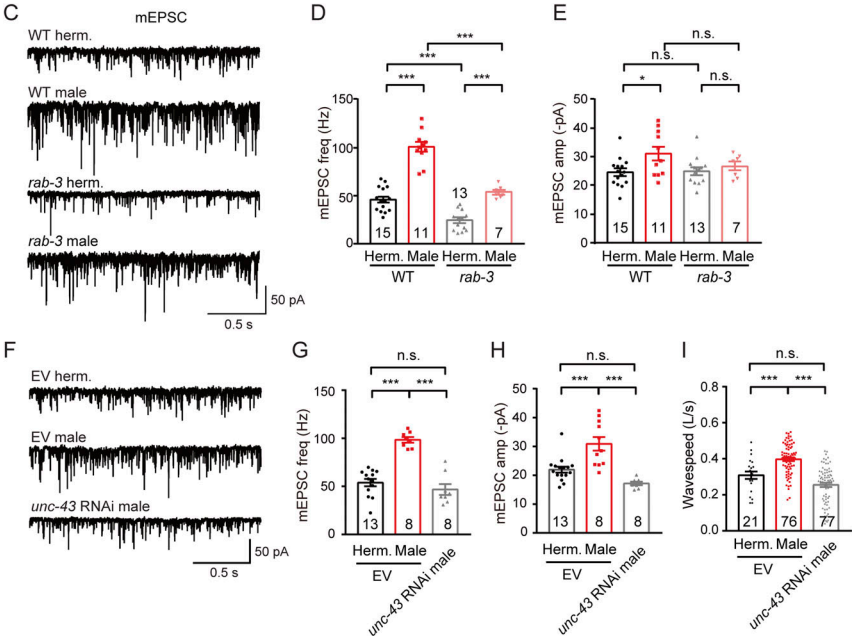

Figure S3. **UNC-43/CaMKII mediates the sexually dimorphic cholinergic transmission. (A and B)** Transcriptome database analysis to identify genes expressed in the cholinergic motor neurons and enriched in males after the L4 stage. **(A)** Venn diagram analysis acquires genes with sex-differential expression during development. Blue: gene group with lower (<10%) or comparable expression in males compared with hermaphrodite during the L3 stage (Kim et al., 2016); red: gene group with higher expression in males compared with hermaphrodite in both the L4-stage and adult stage (Kim et al., 2016); green: gene group expressed in the cholinergic motor neurons (Taylor et al., 2021). Genes with the criteria of P value <0.05 (analyzed with DESeq2 and Likelihood-Ratio tests) and mean counts ≥ 1 are listed. **(B)** Gene list of male-enriched genes after the L4 stage and expressed in the cholinergic motor neurons (208). **(C–E)** *rab-3* mutation cannot block the sexually dimorphic cholinergic transmission at *C. elegans* NMJ. Endogenous acetylcholine transmission was assessed by recording mEPSCs from body-wall muscles of *rab-3* mutant hermaphrodites (Herm.) and males. Representative mEPSC traces (C), the mean mEPSC frequencies (D), and the mean mEPSC amplitudes (E) are shown. The data for WT are the same as in Fig. 1, H and I. In D and E, data are presented as mean values ± SEM. Ns represent the number of animals tested. **(F–H)** Partial knockdown of UNC-43 expression in males reduces cholinergic transmission. Endogenous acetylcholine transmission was assessed by recording mEPSCs from body-wall muscles in males with *unc-43* knockdown (*unc-43* RNAi male). Representative mEPSC traces (F), the mean mEPSC frequencies (G), and the mean mEPSC amplitudes (H) are shown. **(I)** Locomotion behavior analysis of *unc-43* knockdown males (*unc-43* RNAi male). The averaged and individual crawling locomotion velocities were plotted. In D, E, and G–I, data are presented as mean values ± SEM. Ns represent the number of animals tested. One-way ANOVA with post-hoc Bonferroni's multiple comparisons. *P < 0.05, ***P < 0.001, n.s., not significant.

A

Factors	Mutant/treatment	Block
pheromones	*daf-22*	No
hormones	*daf-12*	No
gonadogenesis	*gon-2*	No
spermatogenesis	*fog-2*	No
spermatogenesis	*spe-9*	No
germline proliferation	*glp-1*	No
reproduction	FUdR	No

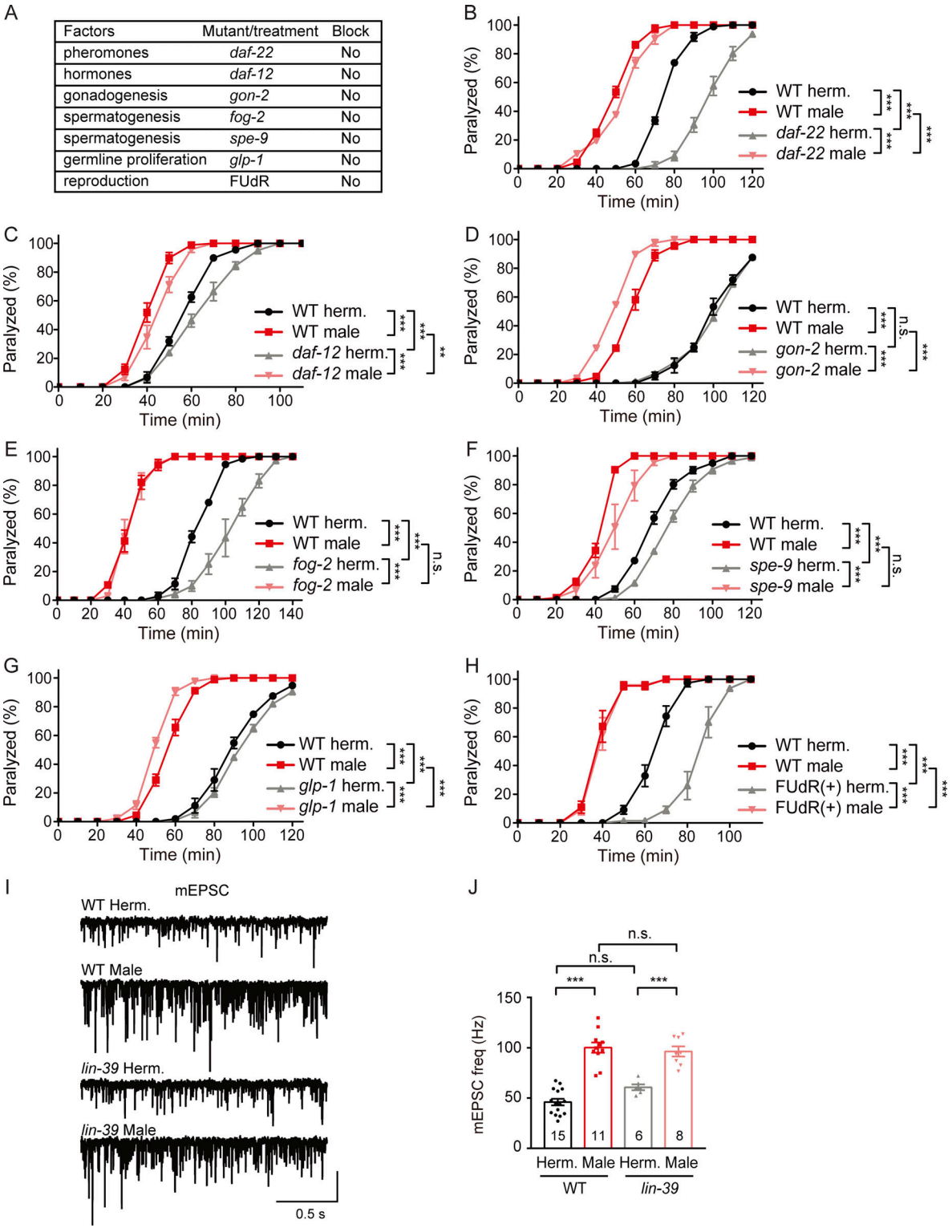

Figure S4. **The sex-specific factors and CA neurons do not mediate the sexually dimorphic cholinergic transmission at NMJs. (A)** The table lists the sex-specific factors examined by mutations or drug treatment and their impact on higher aldicarb sensitivity in males. **(B–G)** Time course analysis of 1.4 mM aldicarb-induced paralysis in hermaphrodites (Herm.) and males with *daf-22* (B), *daf-12* (C), *gon-2* (D), *fog-2* (E), *spe-9* (F), or *glp-1* (G) mutation. **(H)** Time course analysis of 1.4 mM aldicarb-induced paralysis in hermaphrodites and males with 120 µM FUdR treatment. **(I and J)** Endogenous acetylcholine transmission was assessed by recording mEPSCs from body-wall muscles of *lin-39* mutant hermaphrodites (Herm.) and males. Representative mEPSC traces (I) and the mean mEPSC frequencies (J) are shown. The data for WT are the same as in Fig. 1, H and I. In B–H, for each group, $n = 3$ biologically independent samples; each sample contains ≥25 animals. Data are presented as mean values ± SEM. Two-way ANOVA comparing all of the time points. In J, data are presented as mean values ± SEM. Ns represent the number of animals tested. One-way ANOVA with post-hoc Bonferroni's multiple comparisons. ***P < 0.001, n.s. not significant.

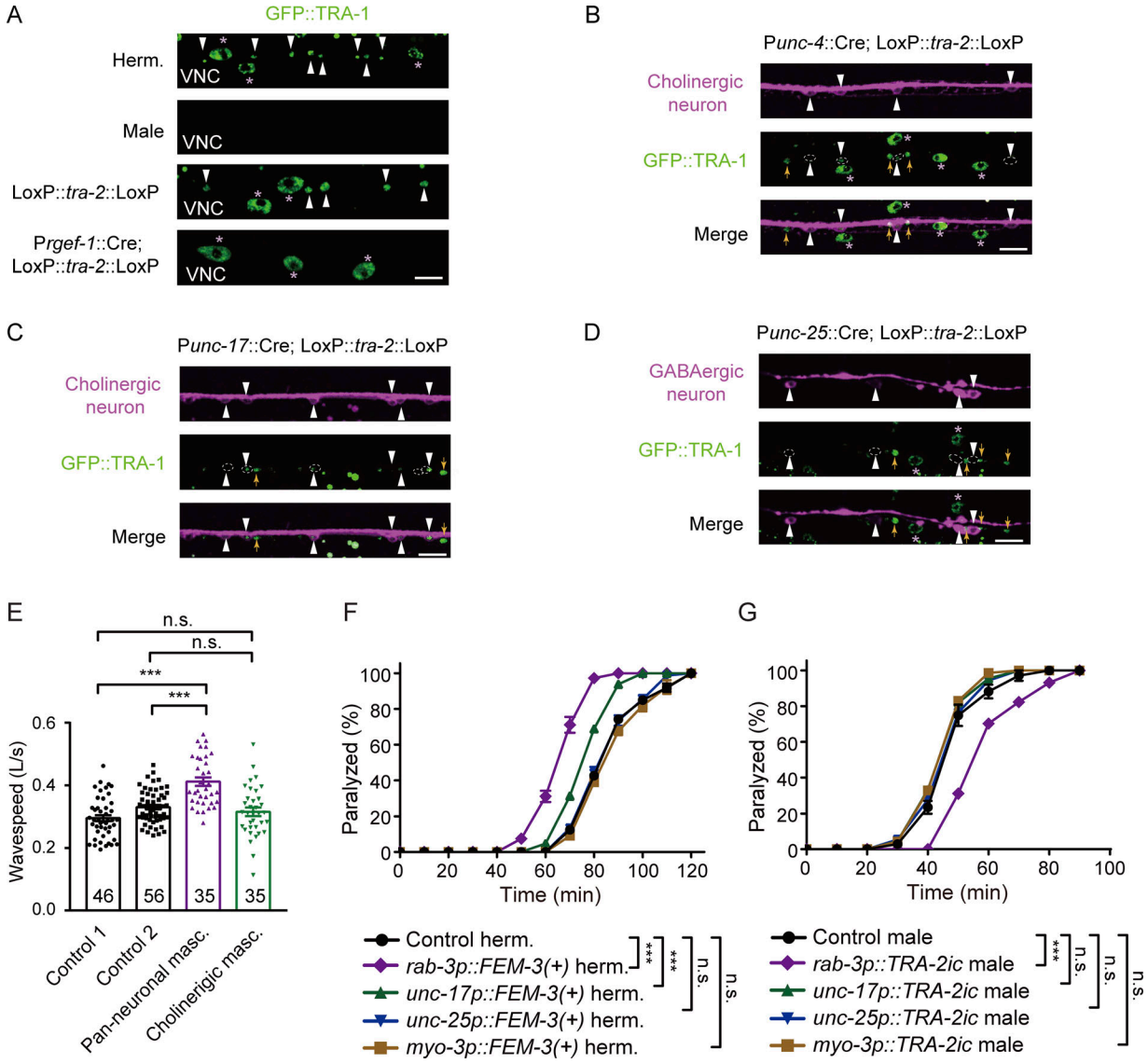

Figure S5. **Conditional knockout of *tra-2* leads to a neuron-specific degradation of TRA-1. (A)** Expression of endogenous GFP::TRA-1 in hermaphrodites, males, and hermaphrodites with pan-neuronal *tra-2* knockout. **(B–D)** Expression of endogenous GFP::TRA-1 in hermaphrodites with *tra-2* specific knockout in cholinergic neurons (B and C) and GABAergic neurons (D). GFP::TRA-1 (green), cholinergic neurons (magenta in B and C, labeled by endogenous UNC-17::mkate2), and GABAergic neurons (magenta in D, labeled by RFP::RAB-3 driven by *unc-25* promoter) are shown. White triangles and white dotted circles indicate cholinergic neurons in B and C and GABAergic neurons in D. Yellow arrows indicate the other neurons. GFP::TRA-1 in muscle cells is marked by asterisks (*). Scale bar, 10 µm. **(E)** Locomotion behavior analysis of hermaphrodites with *tra-2* knockout in all neurons or specifically in cholinergic neurons. The minigene encoding Cre recombinase was driven by the *rgef-1* and *unc-17* promoters to knock out *tra-2* gene in all neurons and cholinergic motor neurons, respectively. For control groups, we used transgenic animals with two loxP sites insertion but without Cre recombinase expression as control 1, and transgenic animals with pan-neuronal Cre recombinase expression, but without two loxP sites insertion as control 2. The averaged and individual crawling locomotion velocities were plotted. **(F)** Time course analysis of 1.4 mM aldicarb-induced paralysis in hermaphrodites expressing FEM-3 in all neurons (under *rab-3* promoter), cholinergic neurons (under *unc-17* promoter), GABAergic neurons (*unc-25* promoter), and muscles (*myo-3* promoters). **(G)** Time course analysis of 1.4 mM aldicarb-induced paralysis in males expressing TRA-2ic in all neurons (under *rab-3* promoter), cholinergic neurons (under *unc-17* promoter), GABAergic neurons (*unc-25* promoter), and muscles (under *myo-3* promoter). In E, data are presented as mean values ± SEM. Ns represent the number of animals tested. One-way ANOVA with post-hoc Bonferroni's multiple comparisons. In F and G, for each of the group, $n = 3$ biologically independent samples; each sample contains ≥25 animals. Data are presented as mean values ± SEM. Two-way ANOVA comparing all of the time points. ***P < 0.001, n.s. not significant.

Provided online are Table S1, Table S2, Table S3, and Table S4. Table S1 shows reagents or resources. Table S2 shows strains. Table S3 shows plasmids and primers. Table S4 shows software and algorithms.